Birch and laminated densified dowels for timber connections - an experimental study

Angelo Aloisio

Angelo Aloisio, PhD
Tenure-Track Assistant Professor
Department of Civil, Architectural and Environmental Engineering
University of L'Aquila, Italy

Current Position
- Tenure-track Assistant Professor (Italy)
- National Scientific Qualification for Associate Professor

Major Research Grant
- FIS-3 Starting Grant
- Italian equivalent of ERC Starting Grant
- Project focus:

Service life, safety, and resilience of engineered wood and bio-based structures under multi-hazards

Research Interests:
- Structural dynamics and vibration-based analysis
- Seismic behavior and multi-hazard resilience
- Advanced modeling of nonlinear structural behavior
- Structural health monitoring and damage detection
- Data-driven and machine learning methods in structural engineering.
- Reliability, uncertainty, and probabilistic assessment

Teaching (Master's Level)
- Masonry Structures
- Structural Monitoring

Titolo: **EXtending the Service Life of Engineered WOOD and Bio-Based Materials under Multi-Hazards**

PI: Angelo Aloisio **Grant**: 1.120.634,70 Euros **Time frame**: 5 years

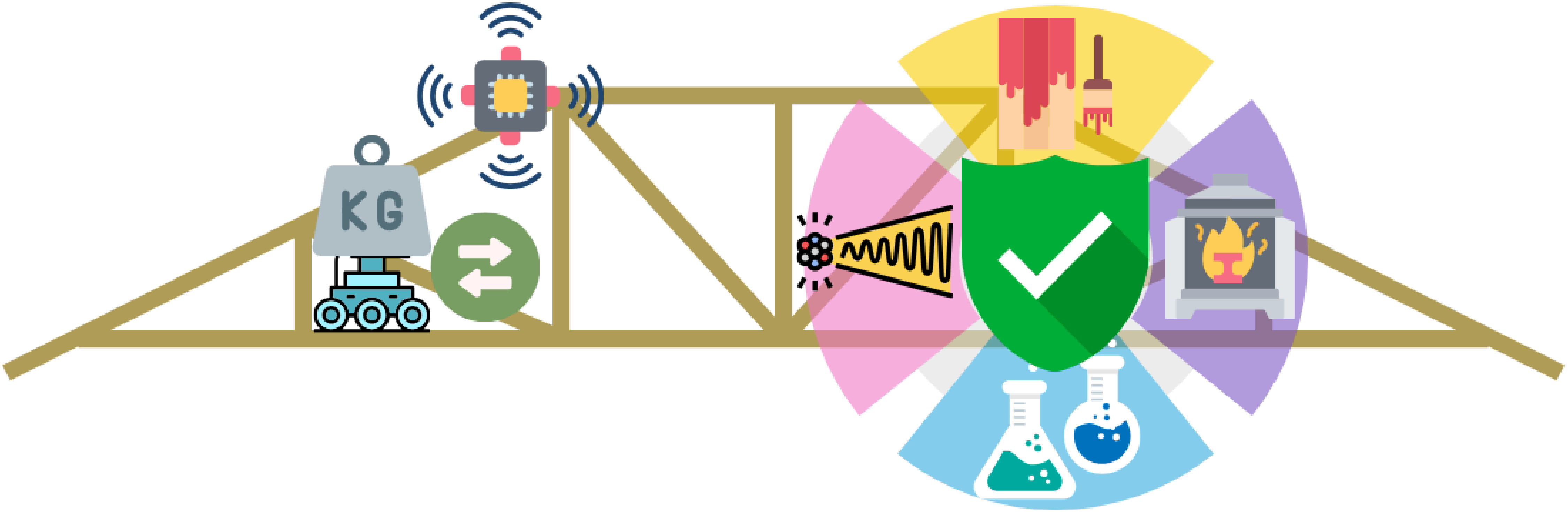

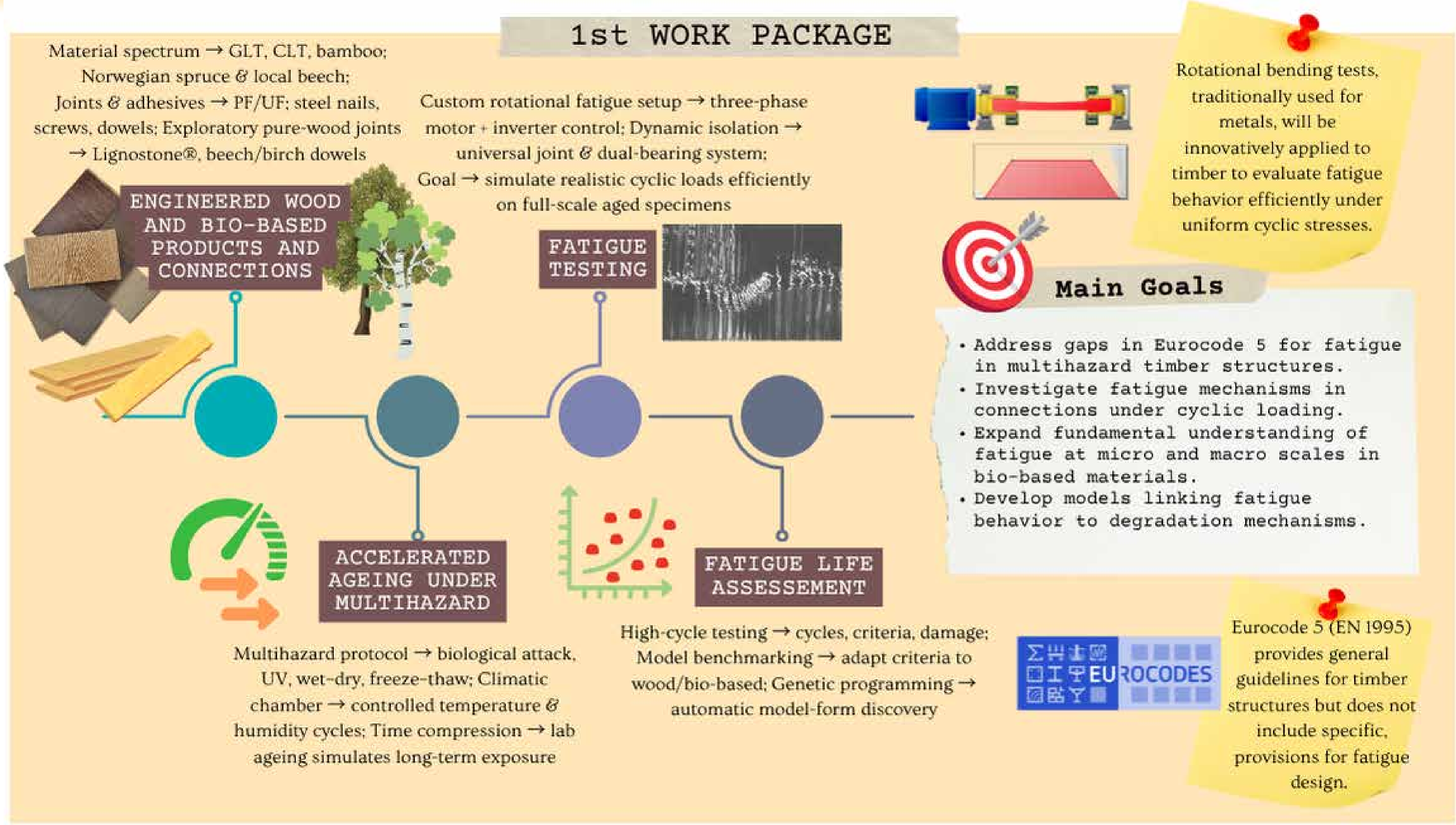
1st WORK PACKAGE
Material spectrum → GLT, CLT, bamboo; Norwegian spruce & local beech; Joints & adhesives → PF/UF; steel nails, screws, dowels; Exploratory pure-wood joints → Lignostone®, beech/birch dowels
ENGINEERED WOOD AND BIO-BASED PRODUCTS AND CONNECTIONS
Custom rotational fatigue setup → three-phase motor + inverter control; Dynamic isolation → universal joint & dual-bearing system; Goal → simulate realistic cyclic loads efficiently on full-scale aged specimens
FATIGUE TESTING
Rotational bending tests, traditionally used for metals, will be innovatively applied to timber to evaluate fatigue behavior efficiently under uniform cyclic stresses.
Main Goals
• Address gaps in Eurocode 5 for fatigue in multihazard timber structures.
• Investigate fatigue mechanisms in connections under cyclic loading.
• Expand fundamental understanding of fatigue at micro and macro scales in bio-based materials.
• Develop models linking fatigue behavior to degradation mechanisms.
ACCELERATED AGEING UNDER MULTIHAZARD
Multihazard protocol → biological attack, UV, wet-dry, freeze-thaw; Climatic chamber → controlled temperature & humidity cycles; Time compression → lab ageing simulates long-term exposure
FATIGUE LIFE ASSESSEMENT
High-cycle testing → cycles, criteria, damage; Model benchmarking → adapt criteria to wood/bio-based; Genetic programming → automatic model-form discovery
EUROCODES
Eurocode 5 (EN 1995) provides general guidelines for timber structures but does not include specific, provisions for fatigue design.

2nd WORK PACKAGE

MULTILEVEL MATERIAL PRESERVATION

Modular preservation → combine copper-based, oil-based & remedial treatments; Targeted delivery → specialized boring pattern preserves structural integrity; Validation → gravimetric analysis, light microscopy, X-ray fluorescence

CHEMICAL MODIFICATION

Furfurylation at scale → improve uniformity & cost with MW-assisted polymerization; Process innovation → faster curing, deeper cell-wall penetration, better reproducibility; Standardization → contribute protocols for chemically modified bio-based materials

THERMAL MODIFICATION

Optimized thermal mod → low-O_2 / N_2 heat treatments; OHT with vaporized vegetable oils; Performance balance → boost durability & stability while minimizing brittleness; Outcome → improved dimensional stability and decay resistance

GAMMA-RAY

Gamma irradiation (Co-60) → controlled, "peaceful nuclear" sterilization; In-situ polymerization → impregnated monomers form durable cross-linked networks; Performance → higher decay/moisture resistance with preserved mechanical properties

AGEING AND FATIGUE (1ST WP)

The last four steps follow the same methodological framework as WP1, ensuring consistency in experimental and analytical approaches.

Main Goals

- Design a modular system with copper, oil, and antifungal treatments for decay prevention.
- Develop a boring pattern for preservative application without structural compromise.
- Optimize heat treatments to enhance durability while minimizing brittleness.
- Improve furfurylation scalability and efficiency with microwave-assisted polymerization.
- establish gamma-ray irradiation as a scalable and environmentally safe preservation technique for structural timber
- Validate performance through accelerated aging and fatigue tests under multihazard conditions.
- Conduct LCA to assess environmental impact and propose sustainable design strategies

3rd WORK PACKAGE

BUILD TWO FULL-SCALE PILOT TRUSSES

Assemble and test two full-scale bio-based trusses, one untreated and one treated, to evaluate multi-hazard performance of various bio-based products, species, and connections.

ACCELERATED AGEING UNDER REPEATED LOADING

Simulate accelearated multi-hazard aging (e.g., freeze-thaw, wet-dry, UV, biological) under repeated loading until failure

STRUCTURAL HEALTH MONITORING AND FATIGUE LIFE ASSESSEMENT

Evaluate SHM data to assess treatment effectiveness, fatigue performance, and moisture monitoring strategies for durability

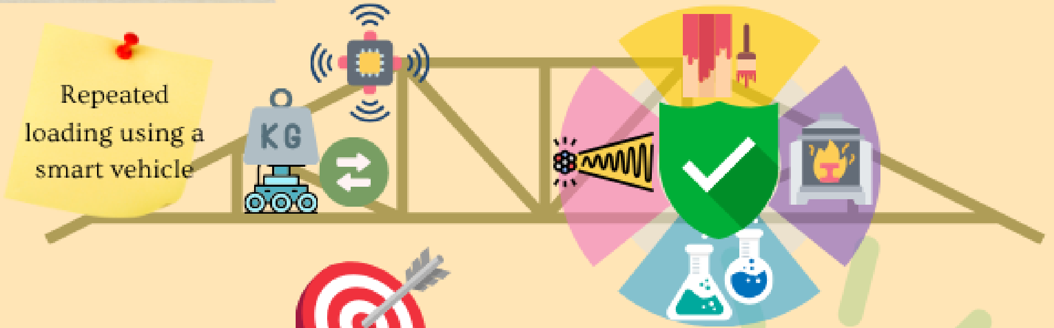

Main Goals

- Build full-scale trusses to study treated vs. untreated bio-based material under multihazard conditions.
- Perform accelerated aging tests on trusses, simulating UV, wet-dry, freeze-thaw, and loads.
- Deploy sensors for real-time SHM and extract samples for CT scan and microstructural analysis.
- Develop a digital twin framework to link SHM data with predictive maintenance strategies.
- Propose unified SHM protocols and Eurocode 5 updates for timber fatigue design.

UV radiation breaks down lignin in wood cell walls, weakening mechanical strength and increasing vulnerability to weathering and decay.

Biological attacks degrade timber by breaking down cellulose and lignin through fungal decay or insect activity

Freeze-thaw cycles cause internal cracking and delamination

Moisture content causes dimensional changes, reducing mechanical strength, and promoting decay and fungal growth

OUTLINE

- **Introduction**
  - Reuse (Sirktre Project);
  - Advantages of Wooden Dowels
- **Theory**
  - FprEN 1995-1-1 model (Modes I-IV);
  - Miller's model (mode V)
- **Experimental test. Discussion and model validation**
  - Embedment test
  - Bending test
  - Axial tension test
  - Shear test
- **Conclusion**

REUSE

Circular Economy

> 180 Milioner NOK

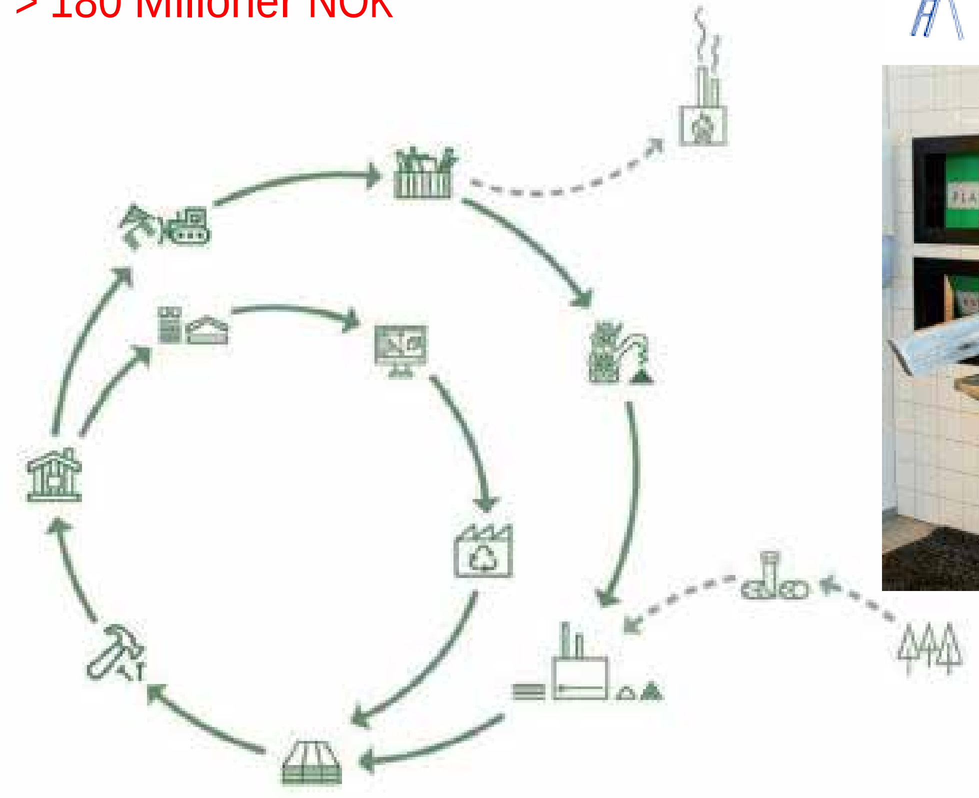

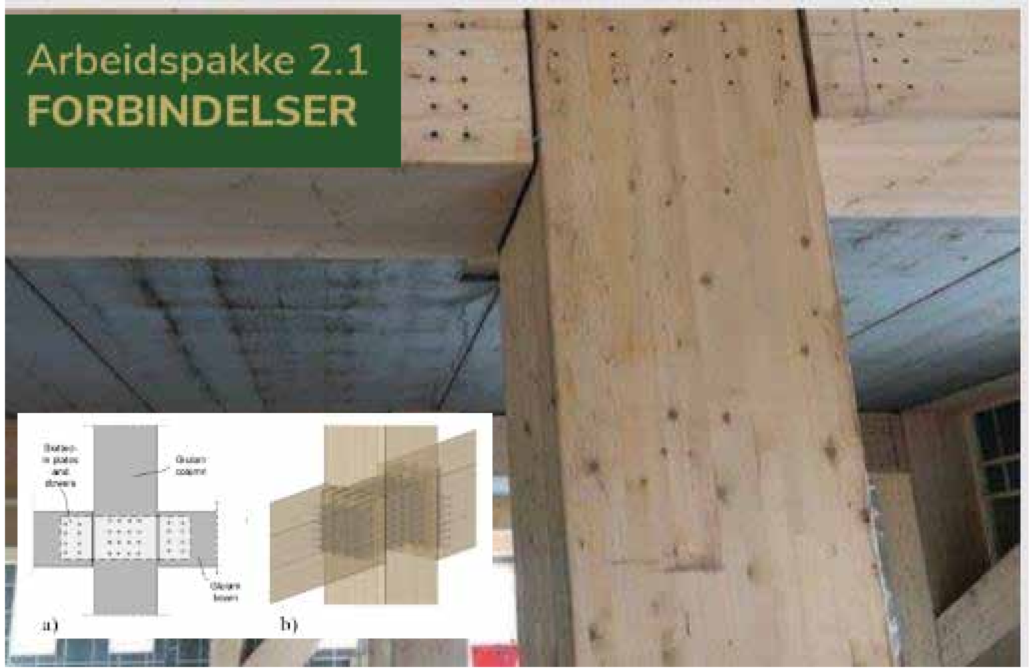

[Picea abies - Norway spruce]

[Fagus sylvatica - European beech]

[Betula spp. - Birches]

Goal: reduce 8% carbon emission in Norway by 2030

Advantages

- Low-carbon, all-wood solution (no steel fasteners or plates)
- Material compatibility: similar stiffness/density to timber → uniform load transfer
- Simple fabrication, reversible/repairable, good for circular design
- Reduced thermal bridging and galvanic/corrosion issues
- Aligns with prEN 1995-1-1 developments on wooden fasteners

Figure: *Wiesenkämper & Berling-Hoffmann*, 2023 Ein Himmelstor aus Holz – Neuer Hangar schafft wirkungsvollen Rahmen für ein Luftschiff in Mülheim. Innsbruck, Austria: Forum Holzwissen,

Angelo Aloisio (angelo.aloisio1@univaq.it)

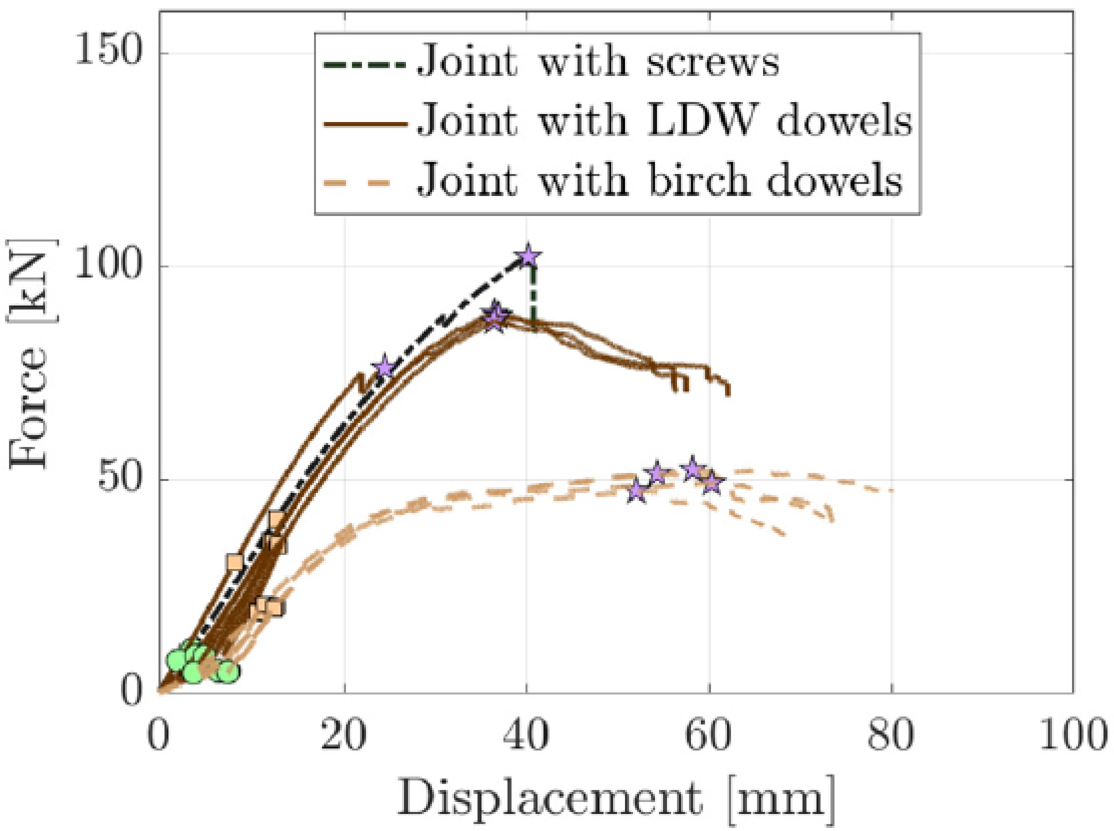
Joint with screws
Joint with LDW dowels
Joint with birch dowels
Force [kN]
Displacement [mm]
0
50
100
150
0
20
40
60
80
100

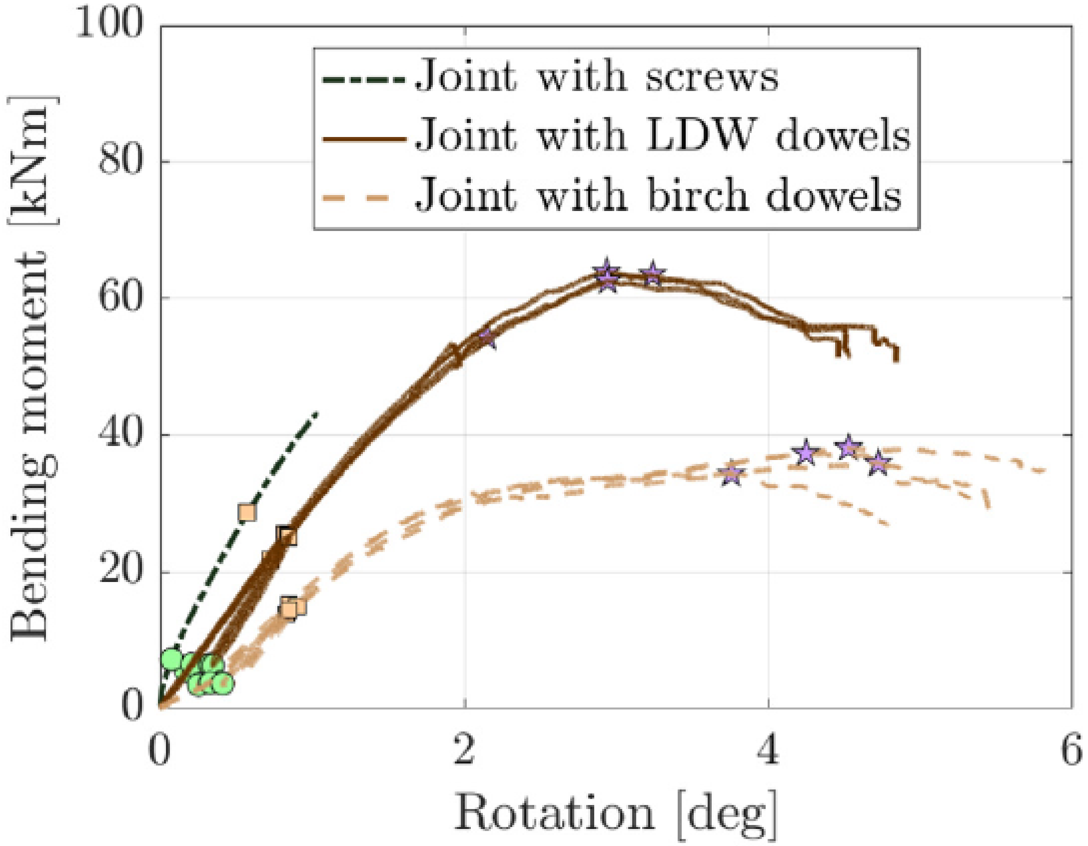
Joint with screws
Joint with LDW dowels
Joint with birch dowels
Bending moment [kNm]
Rotation [deg]
0
20
40
60
80
100
0
2
4
6

1. Theory. Eurocode model

$$
F_{D,k} = \min \begin{cases}
f_{h,1,k} t_{h1} d & \text{(a)} \\
f_{h,2,k} t_{h2} d & \text{(b)} \\
\dfrac{f_{h,1,k} t_{h1} d}{1+\beta}\left[\sqrt{\beta + 2\beta^2\left(1 + \dfrac{t_{h2}}{t_{h1}} + \left(\dfrac{t_{h2}}{t_{h1}}\right)^2\right) + \beta^3\left(\dfrac{t_{h2}}{t_{h1}}\right)^2} - \beta\left(1 + \dfrac{t_{h2}}{t_{h1}}\right)\right] & \text{(c)} \\
\dfrac{f_{h,1,k} t_{h1} d}{2+\beta}\left[\sqrt{2\beta(1+\beta) + \dfrac{4\beta(2+\beta)M_{u,k}}{f_{h,1,k} d t_{h1}^2}} - \beta\right] & \text{(d)} \\
\dfrac{f_{h,1,k} t_{h2} d}{1+2\beta}\left[\sqrt{2\beta^2(1+\beta) + \dfrac{4\beta(1+2\beta)M_{u,k}}{f_{h,1,k} d t_{h2}^2}} - \beta\right] & \text{(e)} \\
\sqrt{\dfrac{2\beta}{1+\beta}}\sqrt{2M_{u,k} f_{h,1,k} d} & \text{(f)}
\end{cases}
$$

- EC5/Johansen assumes ductile plastic hinges in the fastener + wood embedment crushing (great for steel fasteners)
- Adaptations in prEN1995-1-1 (draft): modified embedment formulae and yield/ultimate moment for wooden dowels; still hinge-centric.
- The 1.15 multiplier was reduced to 1.

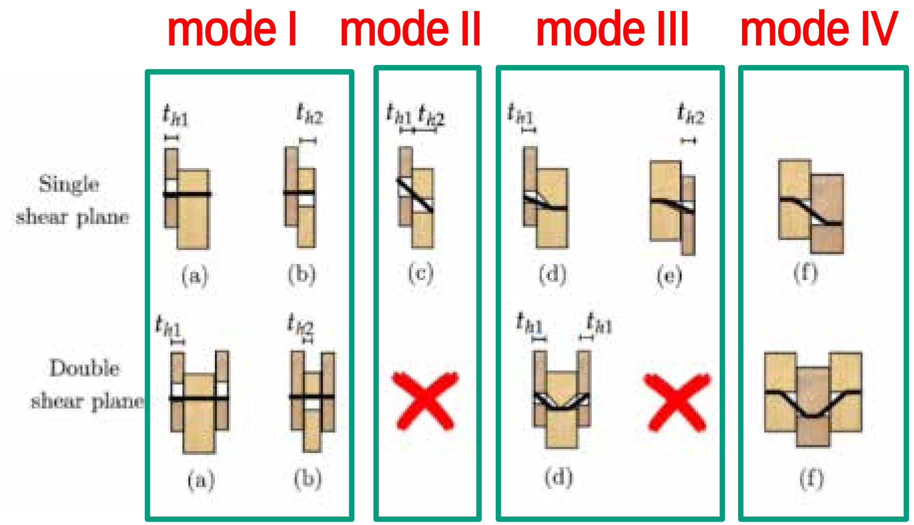

$$M_{u,k} = 0.75\frac{\pi}{32} f_{m,k} d^3 \quad \text{for } 12\text{ mm} \le d \le 30\text{ mm}$$

$$f_{h,k} = 10^{-4}\rho_{dowel,k}\rho_k \frac{1.1(1-0.01d)}{(3.4-0.045d)\sin^2\alpha + \cos^2\alpha}$$

- The prefactor 0.75 corresponds to a reduction factor introduced to account for the brittle behavior of wooden dowels.

1. Introduction. Miller’s model

the brittle failures are different than those provided by Johansen theory (**Sandoli et al 2023**)

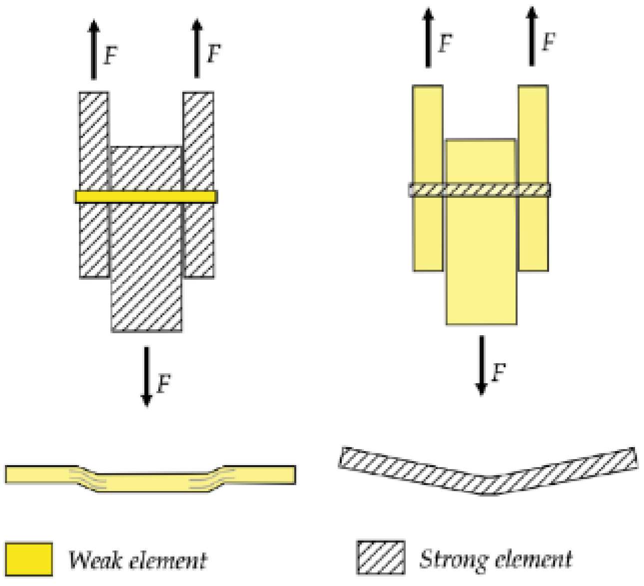

Mode V is introduced (**Miller et al 2010**)

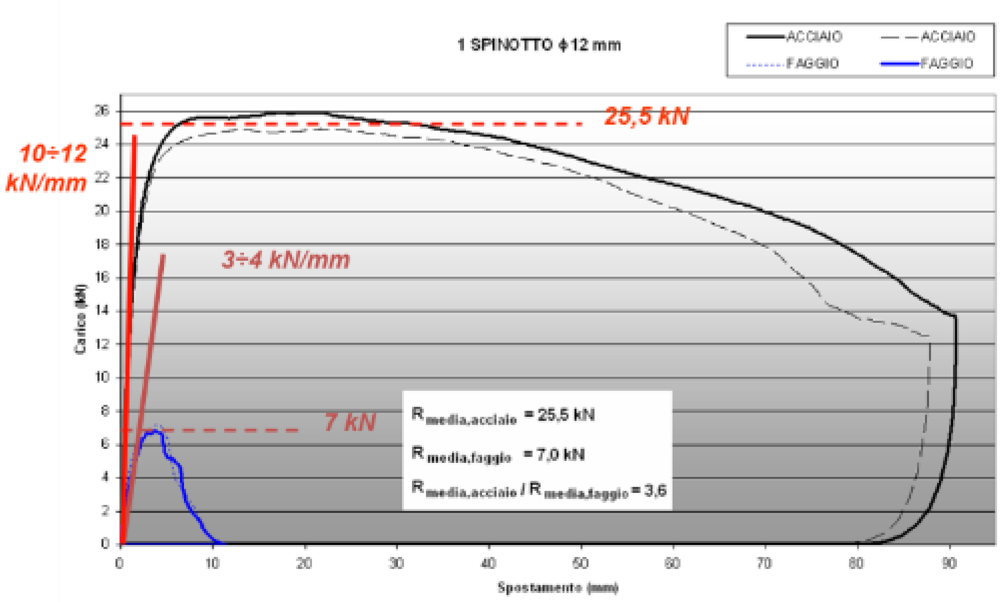

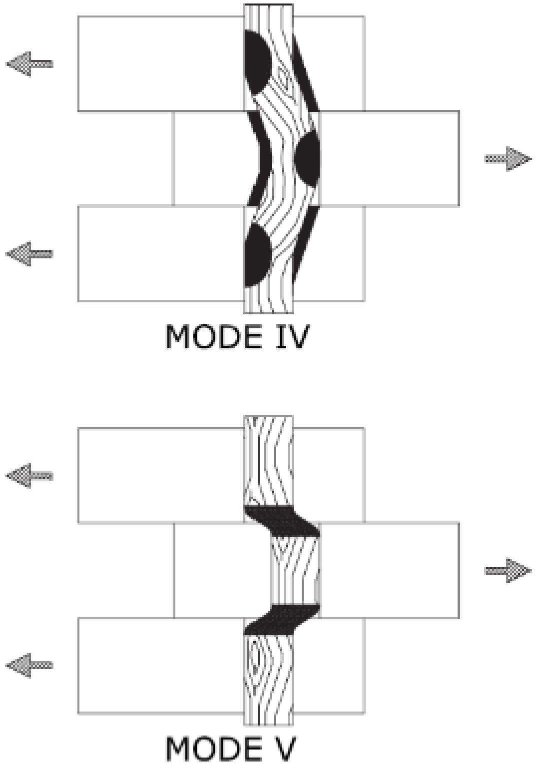

What is it? Combined bending, shear, and compression perpendicular to grain inside the dowel where no plastic hinge forms

Mechanics: distributed longitudinal shear fractures with limited rotation capacity; brittle, span-dependent response.

Why it occurs: dowel and timber have comparable density/stiffness, short unsupported shear span, orthotropic shear strength

1. Introduction. Miller's model

Observations: Multiple longitudinal shear fractures across the dowel; thin intact fibre bundles kinked by flexure. No plastic hinge, span–dependent response

$$f_v = 33.44 G_d G_m^{0.75}$$

shear stress at failure (in N/mm ^{2})

specific gravity of the dowel

$$G_d = \rho_d / \rho_w$$

specific gravity of the embedding material

$$G_m = \rho_m / \rho_w$$

- Regression-based, calibrated for ModeV; not a plastic-hinge (EYM) model;
- Strong dependence on embedment density by construction; some recent tests report weak density influence on yield (Vilguts 2025)
- Sensitive to MC/temperature; use densities compatible with the test or apply corrections.
- A fast, density-driven estimator for shear-dominated dowel failure (Mode V

SHEAR CAPACITY

$$F_v = f_v \cdot A$$

2. Experimental campaign

(a) Half hole setup

(b) Bending setup

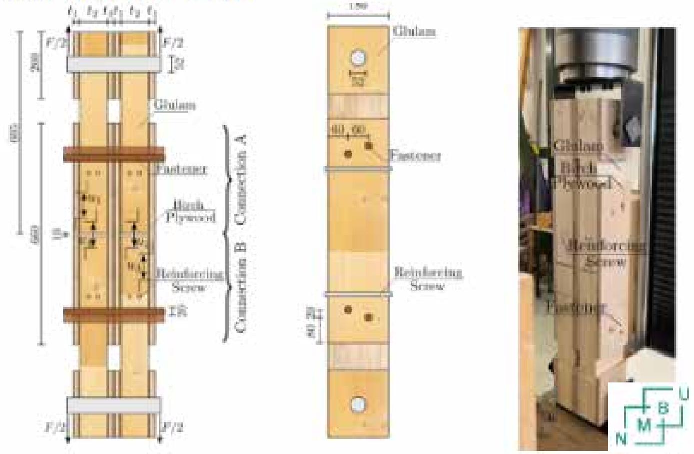

(c) Axial tension test setup

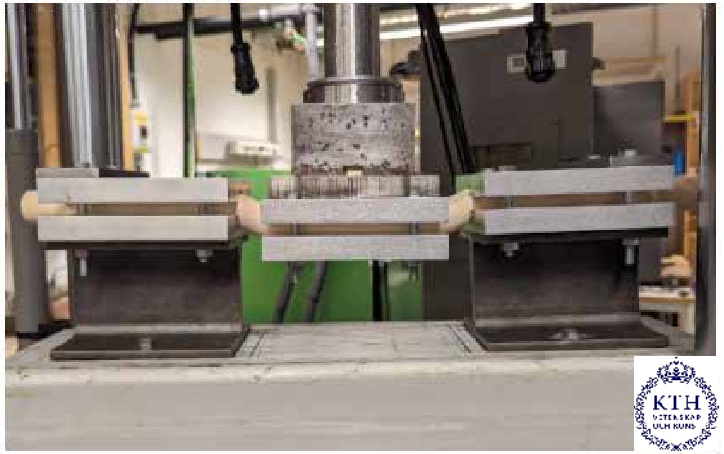

(d) Shear setup

Material (mean values)

Birch dowels (ρ_d = 608 kg/m^3)

LDW dowels (ρ_d = 1350 kg/m^3)

(few more test with steel – screws - and beech connectors were added for comparison)

Birch dowels (ρ_d = 653 kg/m^3)

Beech dowels (ρ_d = 733 kg/m^3)

2. Experimental campaign. Embedment test

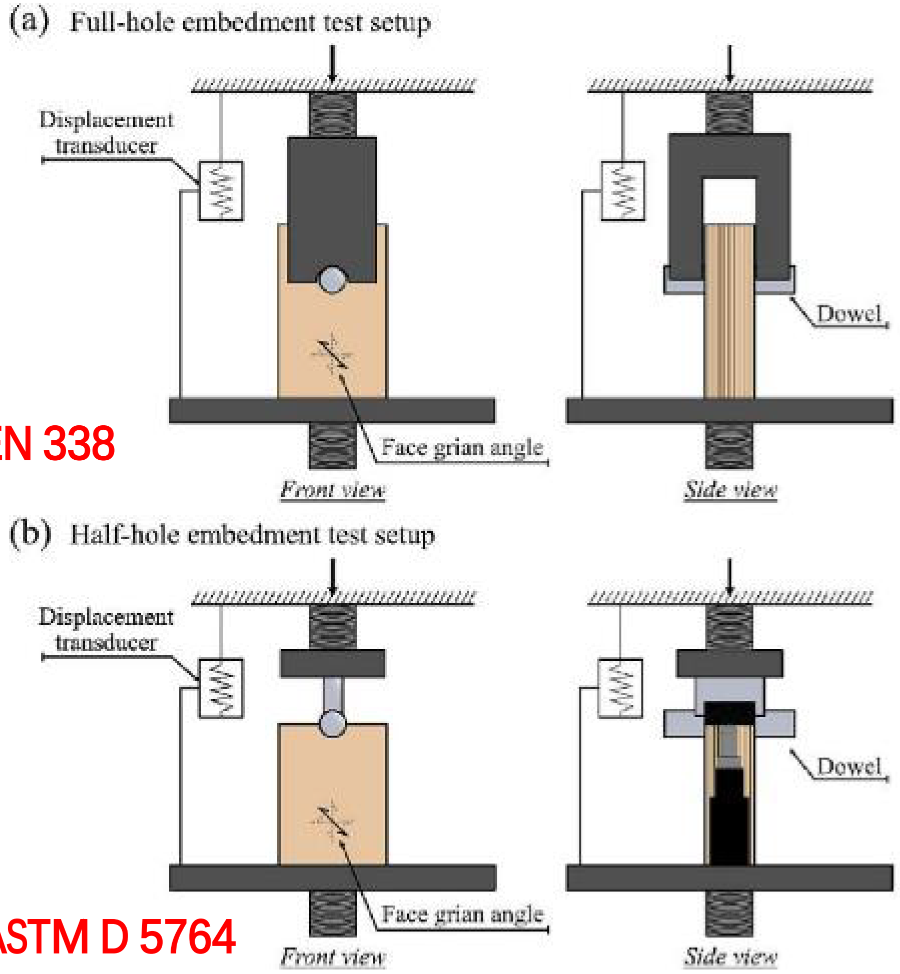

EN 338

ASTM D 5764

Y. Wang et al., Embedment behavior of dowel-type fasteners in birch plywood: Influence of load-to-face grain angle, test set-up, fastener diameter, and acetylation, Construction and Building Materials, Volume 384, 2023,

NOTE Undesired failure mechanism can occur

NOTE: shear behavior instead of grain compression

Teodorescu, B. Pereira, C. Aquino, and J. Branco, "Experimental evaluation of dowel-type timber joints with wooden dowels," Proceedings of the Institution of Civil Engineers: Structures and Buildings, vol. 173, no. 12, pp. 927–938, 2020

NOTE: squeezing of the wooden dowels

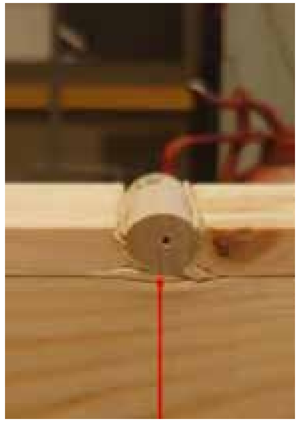

"system strength"

(differs from the bearing behavior between steel dowel and glulam)

half-hole setup is often more suitable !!!

Connection with wooden dowels connectors

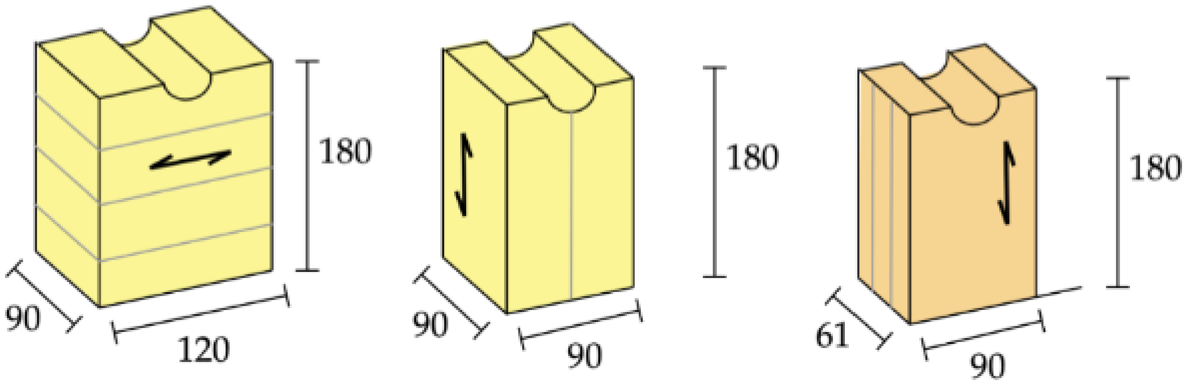

Glulam 90 Glulam 0 Plywood

Material	Dimensions	Repetitions		
		LDW	Birch	Steel
Glulam, 0	90x90x180	10	7	3
Glulam, 90	90x180x120	10	7	3
Plywood	62x90x180	10	7	3

Timber dowel

Steel dowel

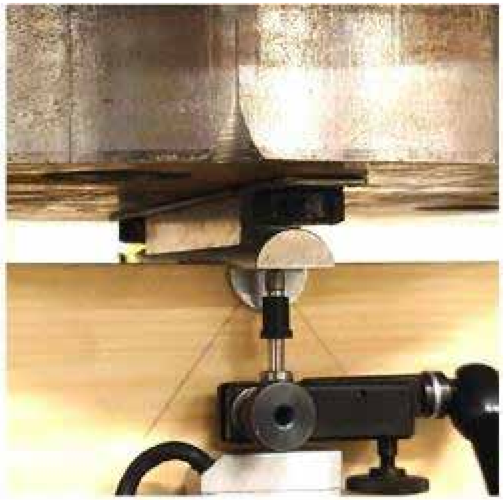

EMBEDMENT TEST

Part of the available material was allocated to conventional embedment tests using steel dowels, which are not affected by this type of deformation and allow for a clearer interpretation of the response. A total of nine embedment test configurations were investigated using the half hole setup

2. Experimental campaign. Embedment test

(a) Half hole setup

Steel and LDW dowels show a two-phase response with an elastic phase followed by plastic behavior

Birch dowels instead show a tri-linear response with distinct hardening: after the initial growth, the curve flattens, then stiffens again until failure (progressive densification of the birch dowel during loading).

Plywood is characterized by significantly higher embedding strength compared to glue laminated timber loaded parallel to the grain

The most **ductile behavior** is obtained loading the glue laminated **timber perpendicularly to the grain**. However, the lowest strengths are associated with this configuration.

2. Experimental campaign. Embedment test

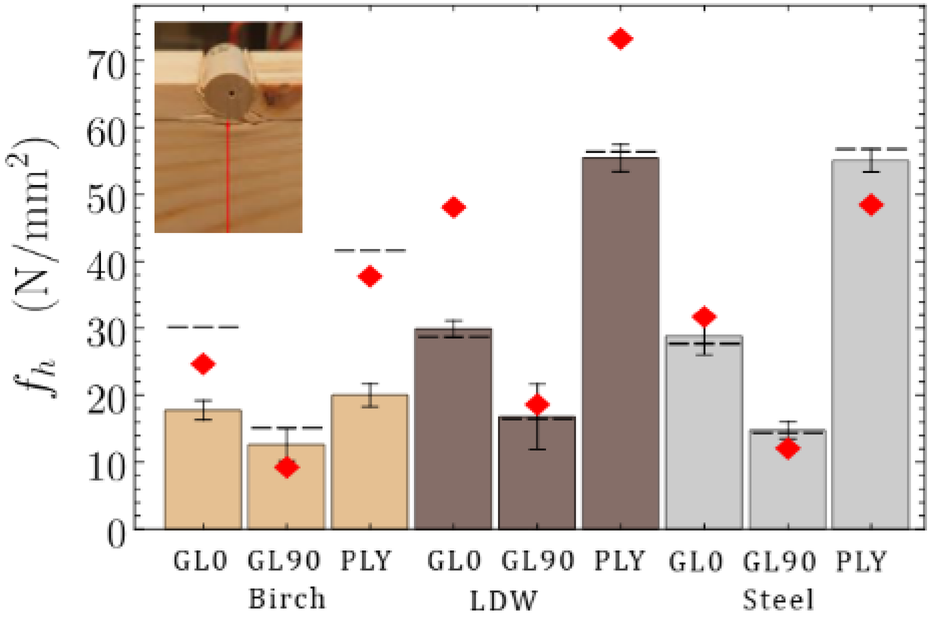

	Name	f_h (N/mm^2)	CoV (%)	$u(f_h)$ (mm)	CoV (%)	$f_{h,EC5}$ (N/mm^2)	$S_{\%}$ (%)
Birch	EMB-GL0-BI	17.8	8%	5.0	0%	25.7	45%
	EMB-GL90-BI	12.6	19%	5.0	2%	10.3	-19%
	EMB-PLY-BI	20.0	9%	5.0	0%	38.9	94%
LDW	EMB-GL0-LDW	29.9	4%	3.3	15%	49.2	65%
	EMB-GL90-LDW	16.8	29%	5.0	0%	19.7	17%
	EMB-PLY-LDW	55.5	4%	5.0	0%	74.4	34%
Steel	EMB-GL0-S	28.9	10%	2.3	9%	32.8	14%
	EMB-GL90-S	14.8	9%	4.8	6%	13.1	-11%
	EMB-PLY-S	55.1	3%	5.0	0%	49.6	-10%

Wooden dowel

$$f_{h,k} = 10^{-4} \cdot \rho_{dowel,k} \cdot \rho_k \cdot \frac{1,1 \cdot (1 - 0,01 \cdot d)}{(3,4 - 0,045 \cdot d) \cdot \sin^2 \alpha + \cos^2 \alpha}$$

$$f_{h,k,Glulam} = \frac{0,082 \cdot (1 - 0,01 \cdot d) \cdot \rho_k}{k_{mat}}$$

$$f_{h,k,PLY} = 0,11 \cdot (1 - 0,01 \cdot d) \cdot \rho_k$$

Steel dowel

Failure modes

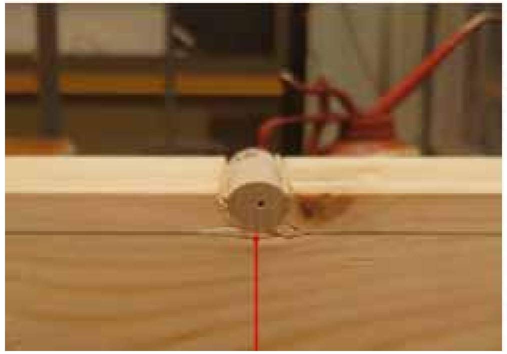

Beech

LDW

Steel

2. Experimental campaign. Bending test

(b) Bending setup

Name	Dowel type	Test type	ρ (kg/m^3)	d (mm)	l (mm)	a (mm)	b (mm)	Test rep. (n°)
BI-D-S	Birch	Shear	618	20	500	70	325	10
BI-D-B	Birch	Bending	599	20	500	155	155	10
LDW-D-S	Laminated densified wood	Shear	1336	20	500	70	325	10
LDW-D-B	Laminated densified wood	Bending	1333	20	500	155	155	10

Name	f_m (N/mm^2)	CoV (%)	τ_v (N/mm^2)	CoV (%)	E (N/mm^2)	CoV (%)	G (N/mm^2)	CoV (%)	Example of failure mode
BI-D-S	143.2	15%	6.8	15%	17820	11%	891	11%	 SHEAR
BI-D-B	132.7	11%	2.9	11%	14639	9%	732	9%	BENDING
LDW-D-S	278.0	7%	13.2	7%	35682	3%	1784	3%	SHEAR
LDW-D-B	235.0	9%	5.1	9%	26580	7%	1329	7%	BENDING

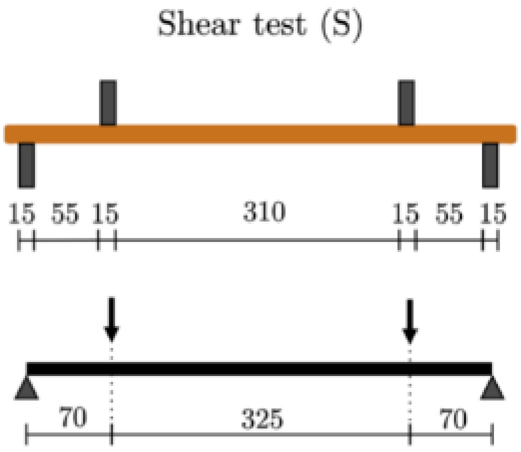

Shear type

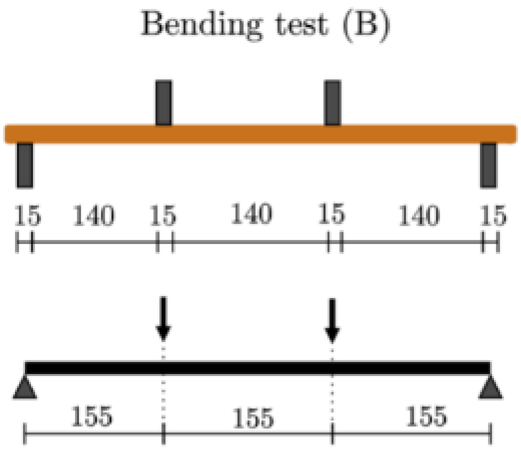

Bending type

In practice, **all dowels failed in bending** in the central portion, regardless of the intended setup, so <u>shear strength could not be assessed</u>.

LDW dowels have much higher bending strength than birch dowels. LDW dowels also displayed significantly higher elastic and shear moduli, with lower coefficients of variation, especially in stiffness-related properties.

2. Experimental campaign. Bending test

BENDING TEST

SHEAR

$$\tau_{max} = \frac{8 \cdot F}{3 \cdot \pi \cdot d^2}$$

BENDING

$$\sigma_{max} = \frac{16 \cdot F \cdot a}{\pi \cdot d^3}$$

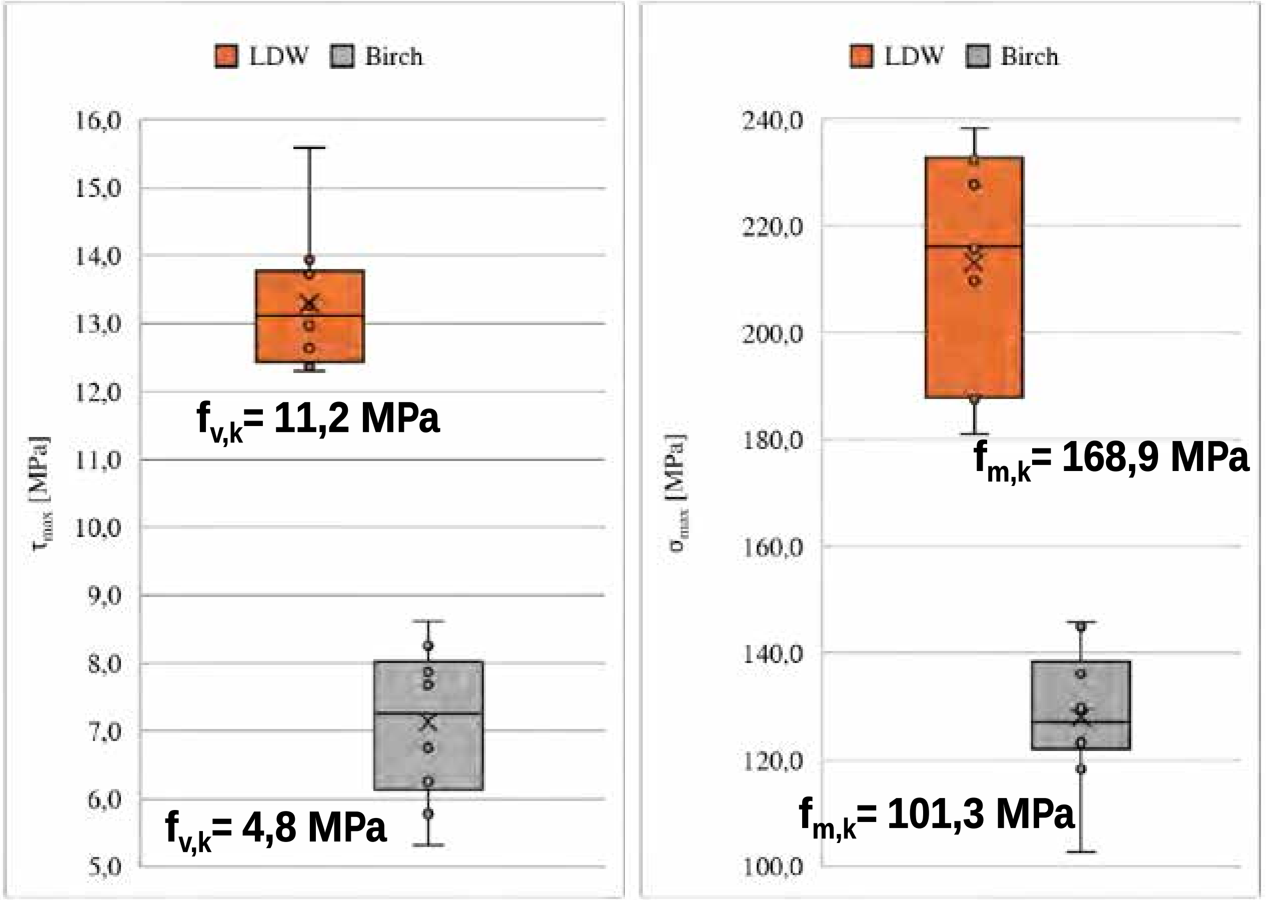

Fpr EN 1995-1-1
11.2.3.4 Connections with wooden dowel

the round or octagonal dowel with 12 mm ≤ d ≤ 30 mm
(diameter of the incircle for octagonal dowel) is made from hardwood:
Beech $f_{m,k}$ = 110 N/mm^2;
Oak $f_{m,k}$ = 60 N/mm^2;
Bongossi $f_{m,k}$ = 100 N/mm^2)

Blaß, H. J.; H. Ernst & H. Werner (1999). “Verbindungen mit Holzstiften: Untersuchungenüber die Tragfähigkeit.” In: BMH Bauen mit Holz 10. Sonderdruck aus bmh 10/99,pp. 1–6

3. Experimental campaign. Tension axial test

PRELIMINARY TEST

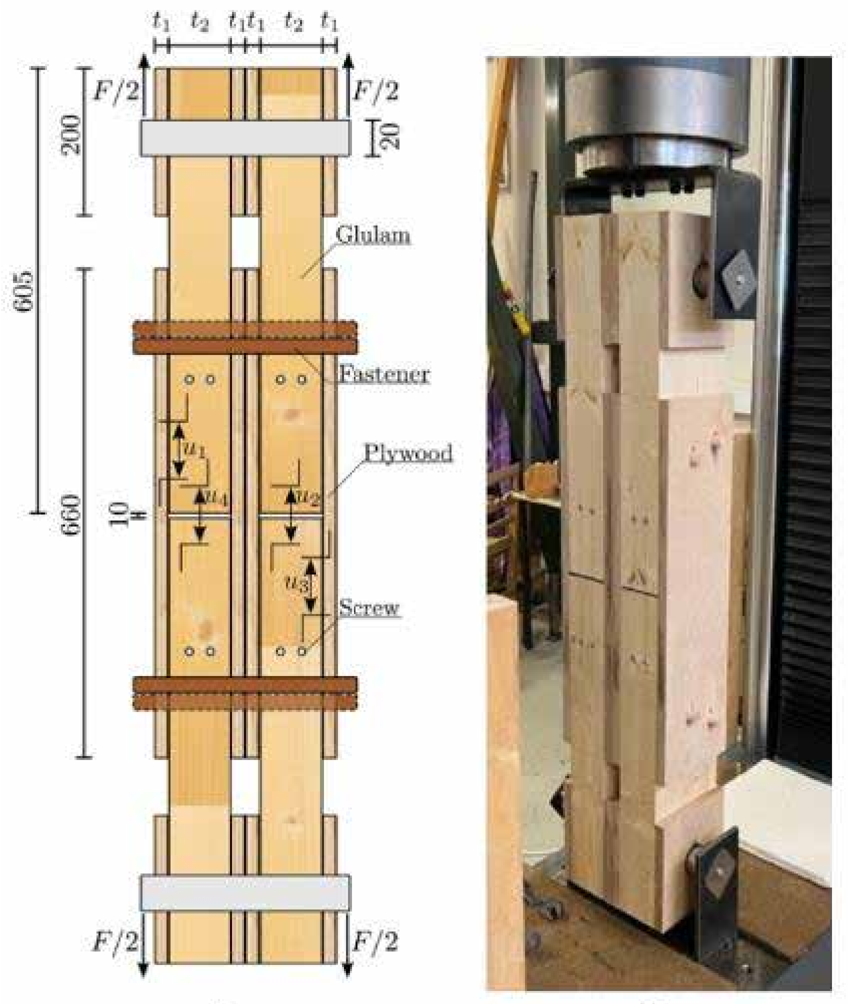

(a) (b)

Birch/beech dowels

Densified wood dowels

Birch Plywood

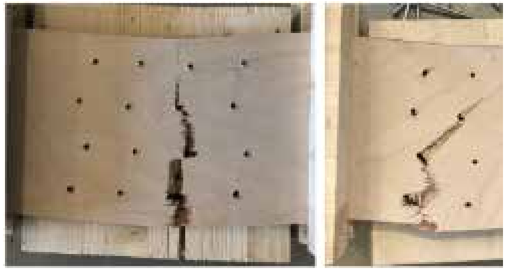

Fully threated screws

Configuration label	Fasteners type	Plates type	Connected members	Shear planes (n°)	Fasteners (n°)
BE-D	Beech dowels	Plywood gusset plates	GL 30c	4	2
BI-D	Birch dowels	Plywood gusset plates	GL 30c	4	2
LDW-D	Laminated densified wood dowels	Plywood gusset plates	GL 30c	4	2
S-S	Steel screws	Plywood gusset plates	GL 30c	4	2

Fasteners type	d (mm)	d_c (mm)	l (mm)	t (mm)	t_1 (mm)	t_2 (mm)	$f_{y,k}$ (N/mm^2)	$M_{y,k}$ (Nm)
Beech dowels	20	-	300	264	21	90	-	-
Birch dowels	20	-	300	264	21	90	-	-
Laminated densified wood dowels	20	-	300	264	21	90	-	-
Steel screws	9	5,9	280	264	21	90	1000	27,2

3. Experimental campaign. Tension axial test

PRELIMINARY TEST

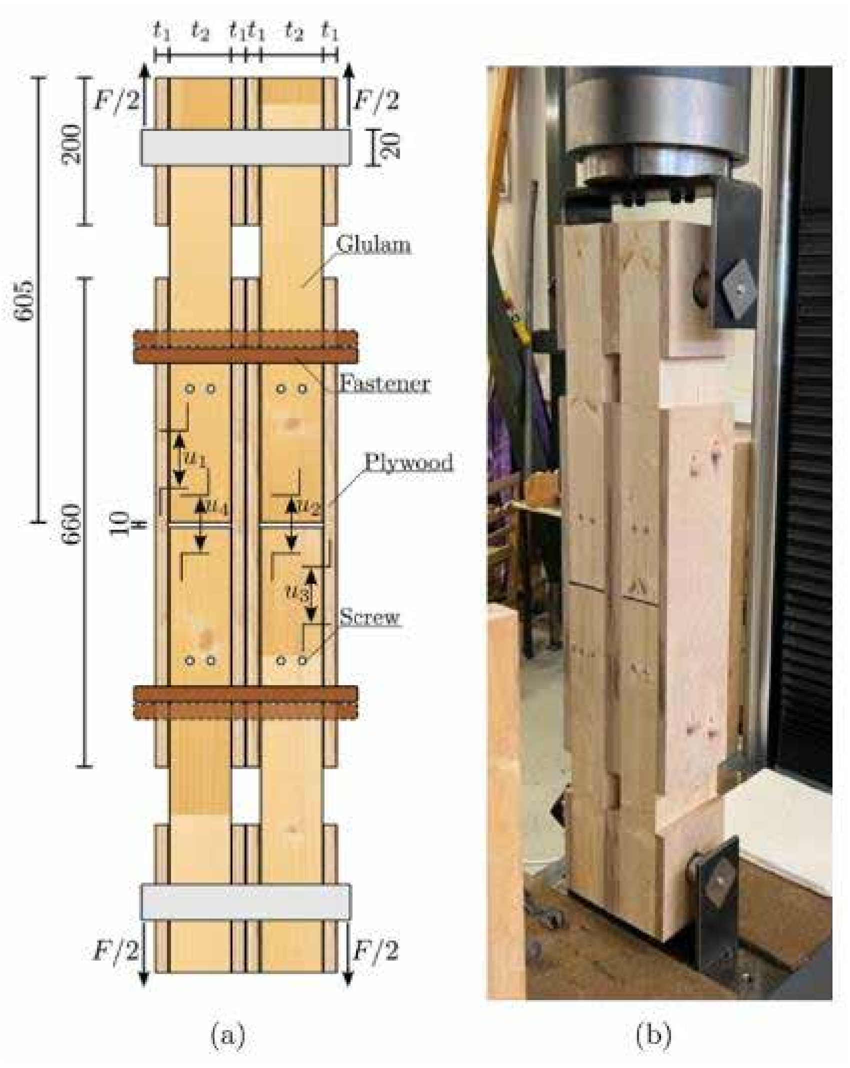

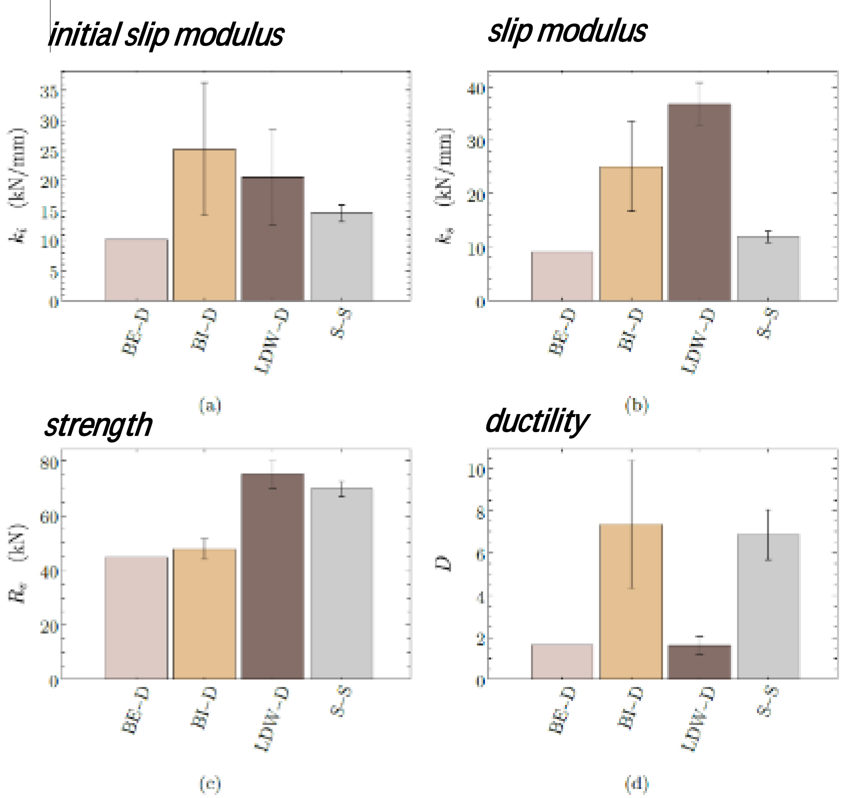

20 mm densified wood dowel showed similar short-term capacity compared to 9 mm steel screws.

3. Experimental campaign. Tension axial test

PRELIMINARY TEST

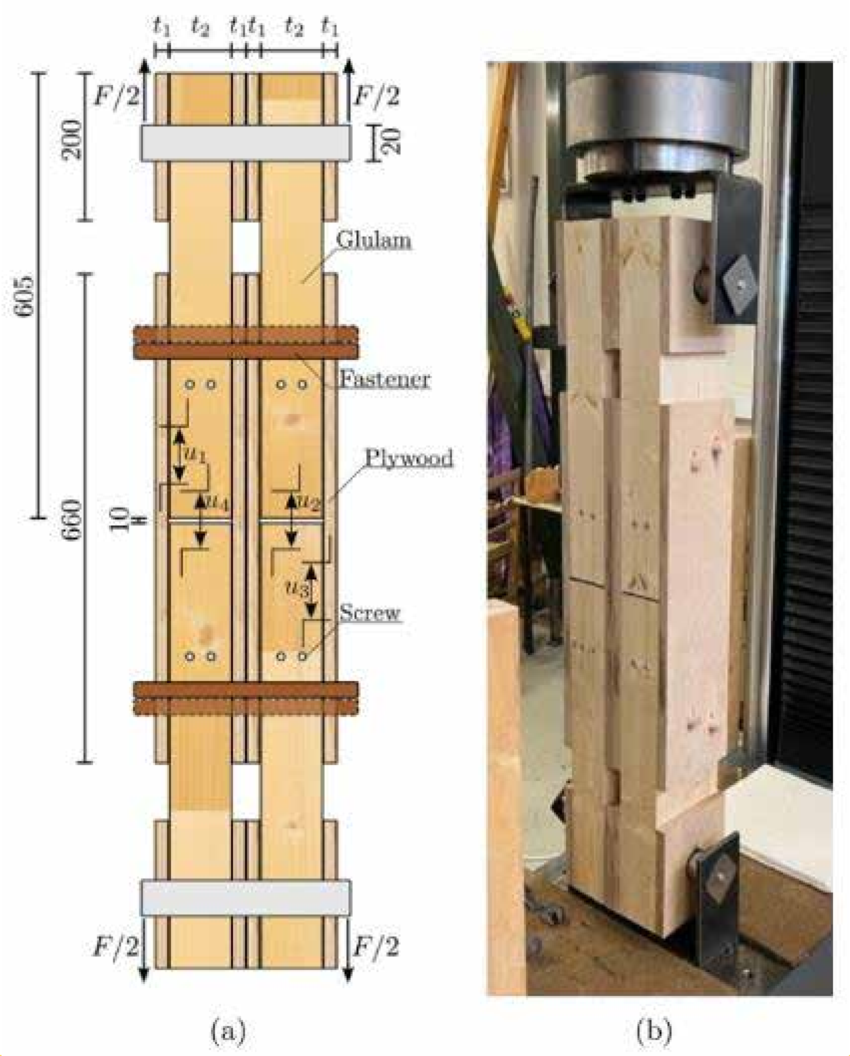

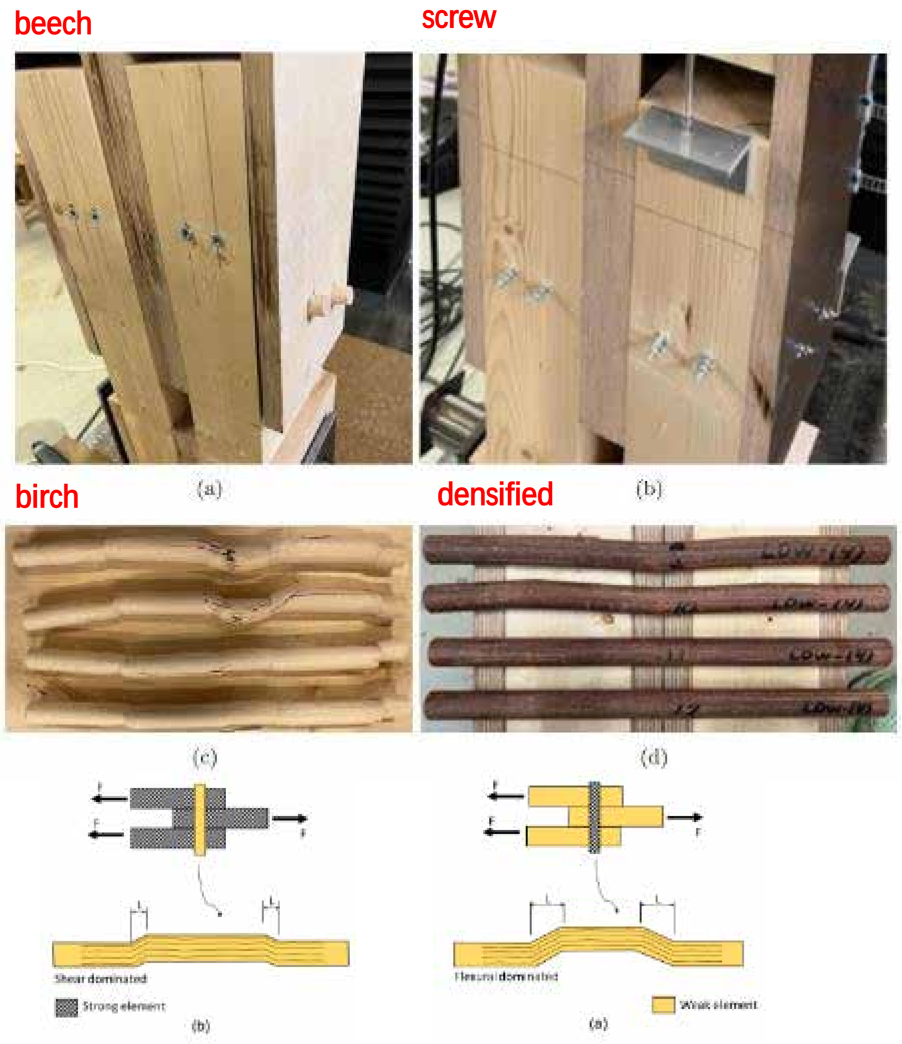

Mode V is observed (**Miller et al 2010**)

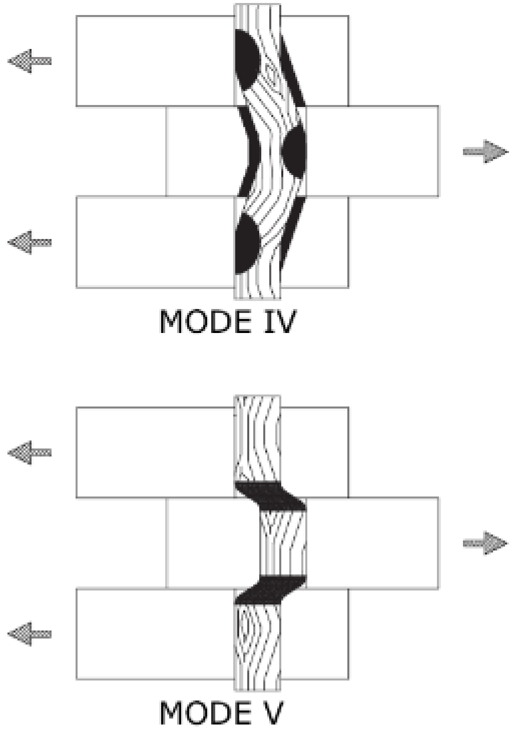

the brittle failures are different than those provided by Johansen theory (**Sandoli et al 2023**)

3. Experimental campaign. Tension axial test

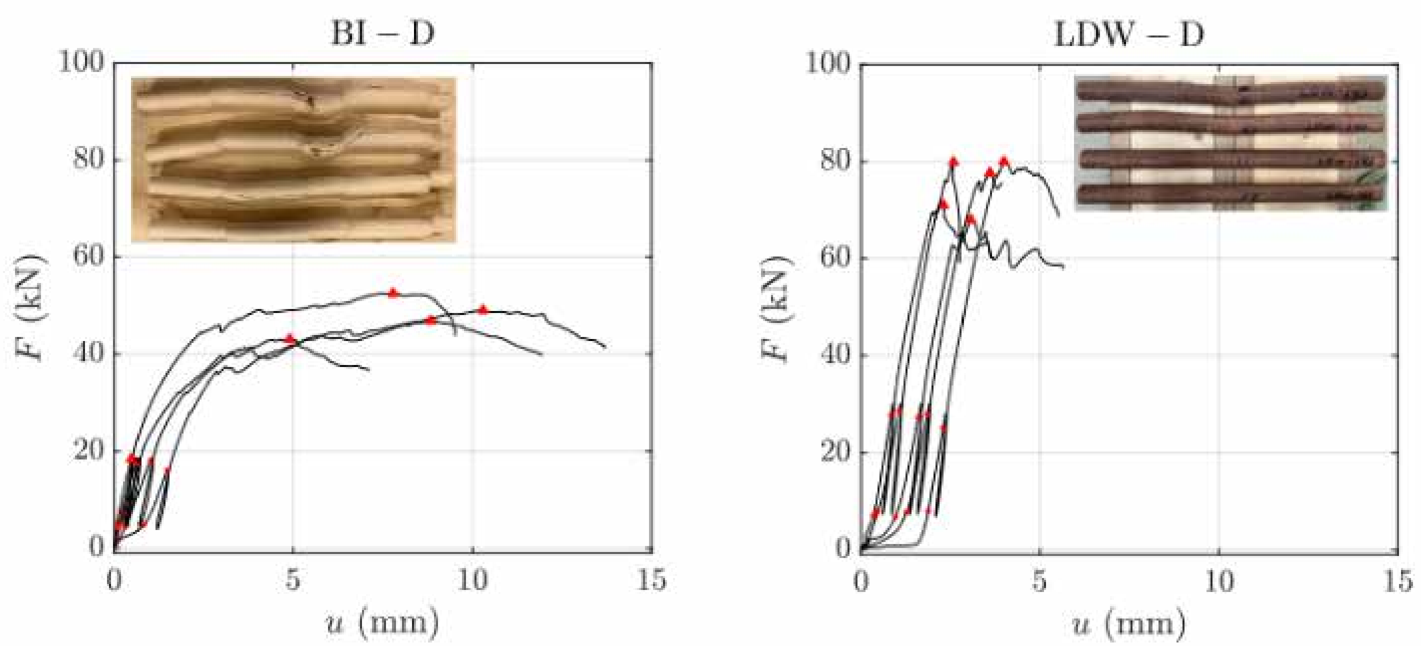

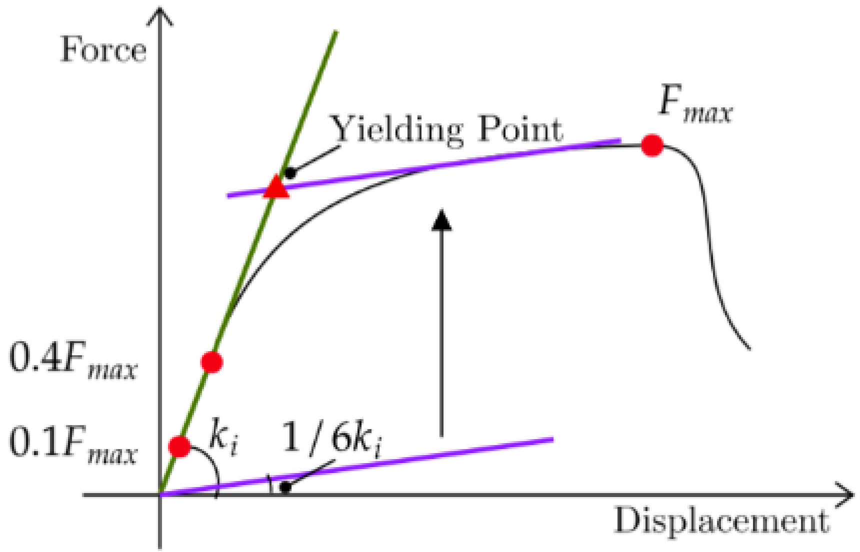

BI-D				LDW-D			
Config.	R_y (kN)	u_u (mm)	D	Config.	R_y (kN)	u_u (mm)	D
BI-D-1	52.5	7.8	10.0	LDW-D-1	71.0	2.3	2.0
BI-D-2	49.1	10.3	5.3	LDW-D-2	79.9	2.6	1.1
BI-D-3	46.9	8.8	7.2	LDW-D-3	80.0	4.0	1.6
BI-D-4*	18.4	0.5	–	LDW-D-4	77.7	3.6	1.2
BI-D-5	43.1	4.9	6.9	LDW-D-5	68.0	3.1	2.1
Avg.	**47.9**	**8.0**	**7.3**	Avg.	**75.3**	**3.1**	**1.6**
CoV	7%	25%	23%	CoV	7%	20%	25%

Beech and birch dowels with capacities around 40 kN, and LDW and screws with nearly double that.

In terms of ductility, birch and screws were the most ductile, while beech and LDW were the least.

3. Experimental campaign. Tension axial test

Experimental vs. predicted capacity values (Eurocode 5)

Label	$R_{v,exp}$ per dowel [kN]	$R_{v,prEC5}$ [kN]	Rel. Error [%]	$R_{v,prEC5,exp}$ [kN]	Rel. Error [%]
BI-D-1	6.56	8.43	28	6.63	1
BI-D-2	6.14	8.43	37	6.63	8
BI-D-3	5.86	8.43	44	6.63	13
BI-D-4*	2.30	8.43	267	6.63	188
BI-D-5	5.39	8.43	56	6.63	23
Mean	**5.99**	**8.43**	**42**	**6.63**	**11**
LDW-D-1	8.88	16.925	91	13.08	47
LDW-D-2	9.99	16.925	69	13.08	31
LDW-D-3	10.00	16.925	69	13.08	31
LDW-D-4	9.71	16.925	74	13.08	35
LDW-D-5	8.50	16.925	99	13.08	54
Mean	**9.42**	**16.93**	**81**	**13.08**	**39**

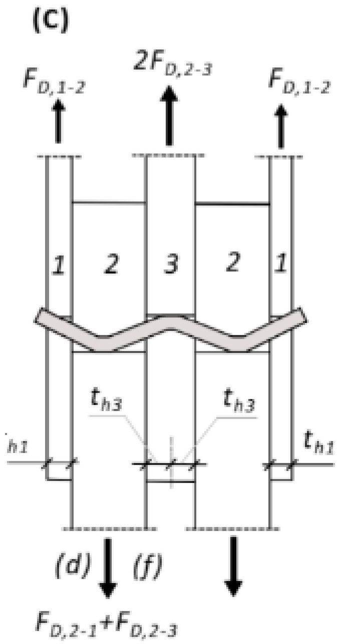

experimental vs Eurocode 5 embedment values

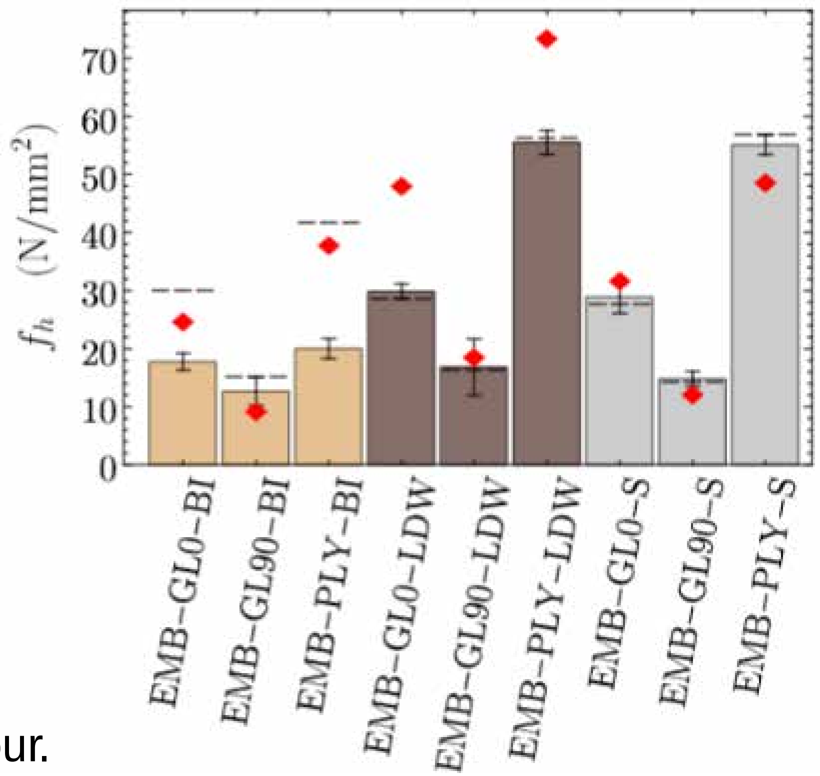

- The experimental shear capacity was divided by the number of shear planes, four.
- Predictions were calculated using both theoretical embedment strength, giving $R_{v\ prEC5}$, and experimental embedment values, giving $R_{v\ prEC5\ exp}$
- The governing mechanism was failure mode C according to Fig. 11.8 of FprEN 1995-1-1 (2025).

3. Experimental campaign. Tension axial test

Experimental vs. predicted capacity values (Miller)

Label	$R_{v,y,\text{exp}}$ per dowel [kN]	f_v Miller [MPa]	$R_{v,y,\text{sim}}$ Miller [kN]	Rel. Error [%]
BI-D-1	5.21	15.22	3.46	-34%
BI-D-2	4.55	15.22	3.46	-24%
BI-D-3	3.98	15.22	3.46	-13%
BI-D-4*	4.74	15.22	3.46	-27%
BI-D-5	4.56	15.22	3.46	-24%
Mean	**5.99**	**15.22**	**3.46**	**-24%**
LDW-D-1	8.88	33.43	7.61	-14%
LDW-D-2	9.99	33.43	7.61	-24%
LDW-D-3	10.00	33.43	7.61	-24%
LDW-D-4	9.71	33.43	7.61	-22%
LDW-D-5	8.50	33.43	7.61	-11%
Mean	**9.42**	**33.43**	**7.61**	**-19%**

shear stress at failure (in N/mm ^{2})

$$f_v = 33.44 G_d G_m^{0.75}$$

$G_d = \rho_d/\rho_w$ specific gravity of the dowel

$G_m = \rho_m/\rho_w$ specific gravity of the emb. material

$$F_v = f_v \cdot A$$

SHEAR CAPACITY

- The experimental shear capacity was divided by the number of shear planes, four.
- In contrast to EC5 model, Miller's model is conservative, and its predictive accuracy is much better

Experimental campaign at NMBU. Main takeaways:

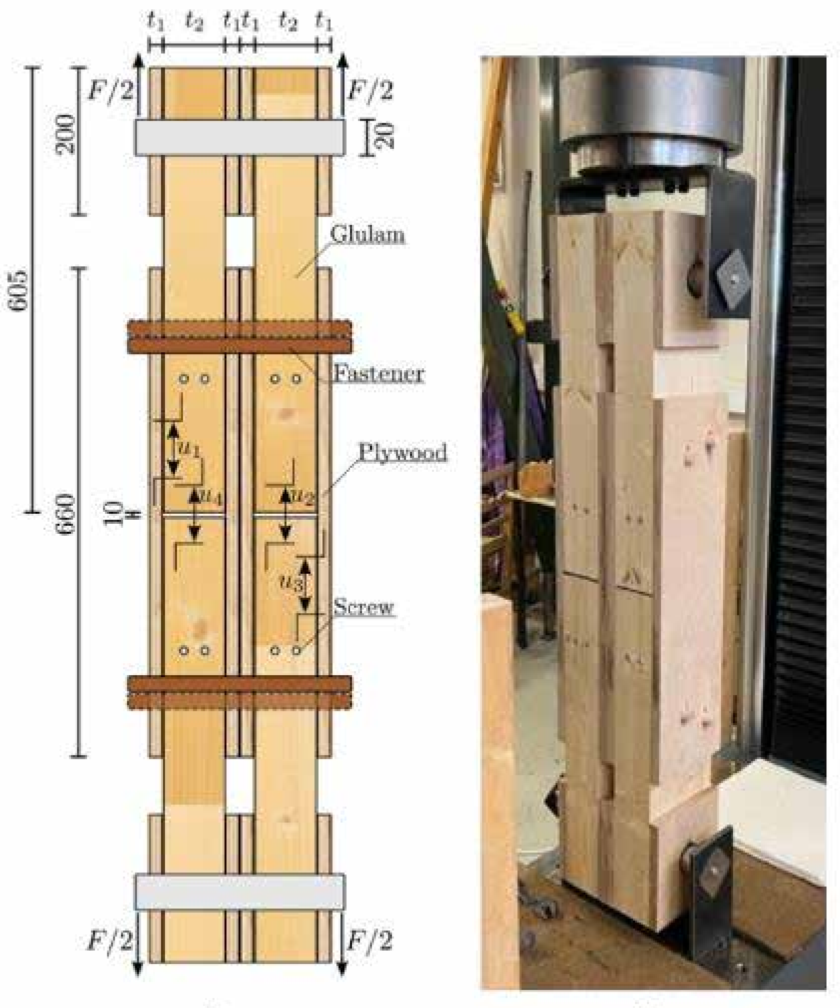

(a) (b)

- **Experimental observation**: Wooden dowels fail mainly by a Mode V bending–shear mechanism: brittle, span–dependent, no plastic hinge.
- **Fpr 1995-1-1**:
  - (i) Gives reasonable ranking for capacity, but its physics (plastic hinges in the fastener) does not match Mode V in wood dowels.
  - (ii) The main error source is the embedment formulation for wood–wood contact; code values tend to overestimate capacity.
  - (iii) Even with measured embedment, EYM remains optimistic because it ignores the bending–shear interaction and short shear span.
- **Miller**:
  - (i) Density-driven regression calibrated for Mode V; easy to use but showed larger errors (bias/dispersion) on our data.
  - (ii) Highly sensitive to embedment density and service conditions

4. KTH Experimental campaign. Shear test

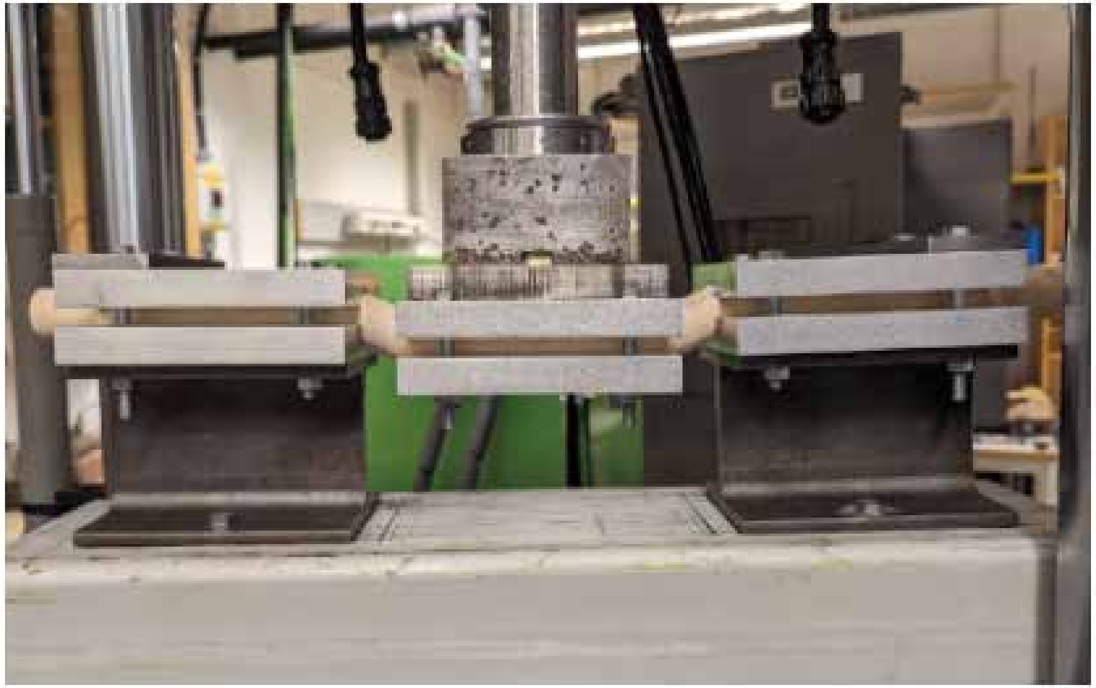

(d) Shear setup

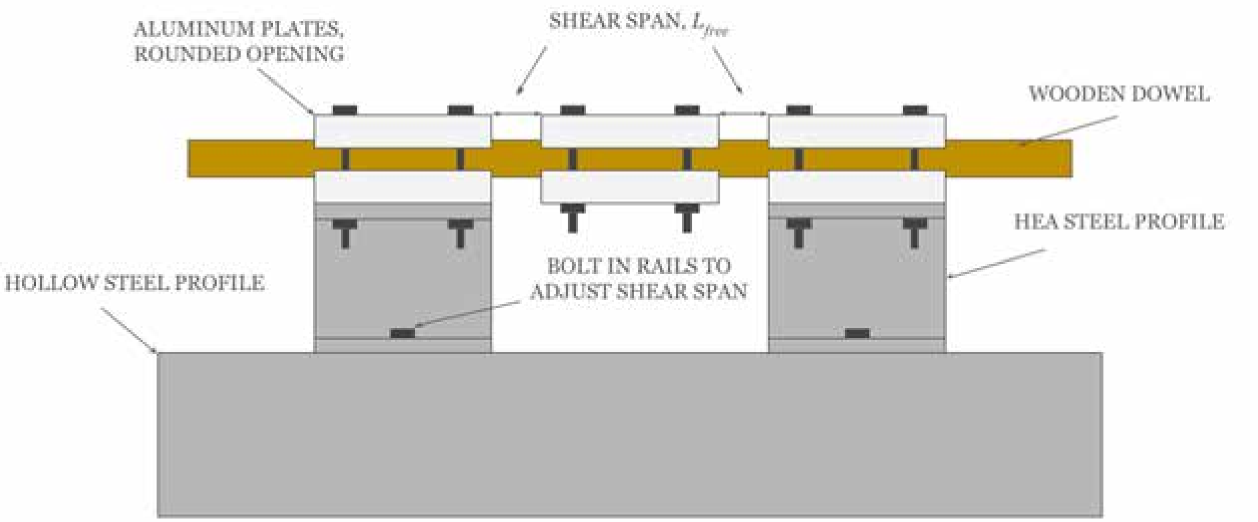

specially designed aluminium device

- Previous tests showed that wooden dowels mainly fail through type V mechanisms.
- The embedment and bending tests confirmed that standard setups for steel dowels are not suitable for deriving the parameters required by the European Yield Model

4. KTH Experimental campaign. Shear test

Geometrical details of the test groups.

Group	Species	Diameter d (mm)	Length L (mm)
B20	Birch	20	600
B30	Birch	30	600
E20	Beech	20	500

Each test replicate was labeled with a unique code L-S/S-DD-XX-Y as shown in Table

Field	Example	Meaning
L	R / T	Loading direction: R = radial, T = tangential
S/S	0/1, 1/2, 1/1	Shear-span ratio L_{free}/d: 0, 0.5, or 1.0
DD	20, 30	Nominal dowel diameter (mm)
XX	BI, BE	Species: BI = birch, BE = beech
Y	1–5	Specimen sequence number

Two hardwood species were tested

Birch dowels (ρ_d = 653 kg/m^3)
Beech dowels (ρ_d = 733 kg/m^3)
(mean values)

different shear-span level, with L_{free}/d equal to 0 (no span), 0.5, and 1.0;

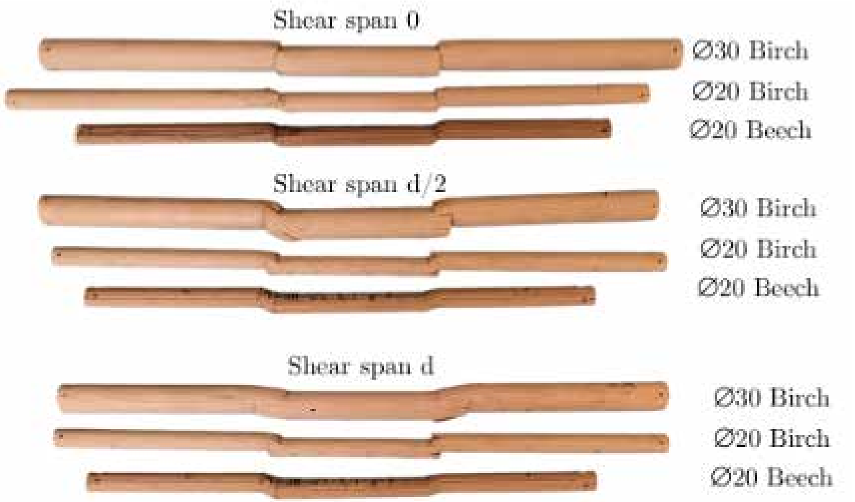

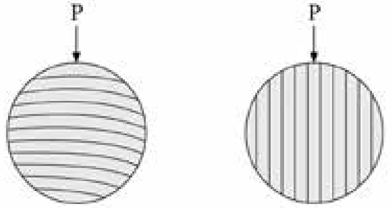

radial and tangential loading directions

4. KTH Experimental campaign. Shear test

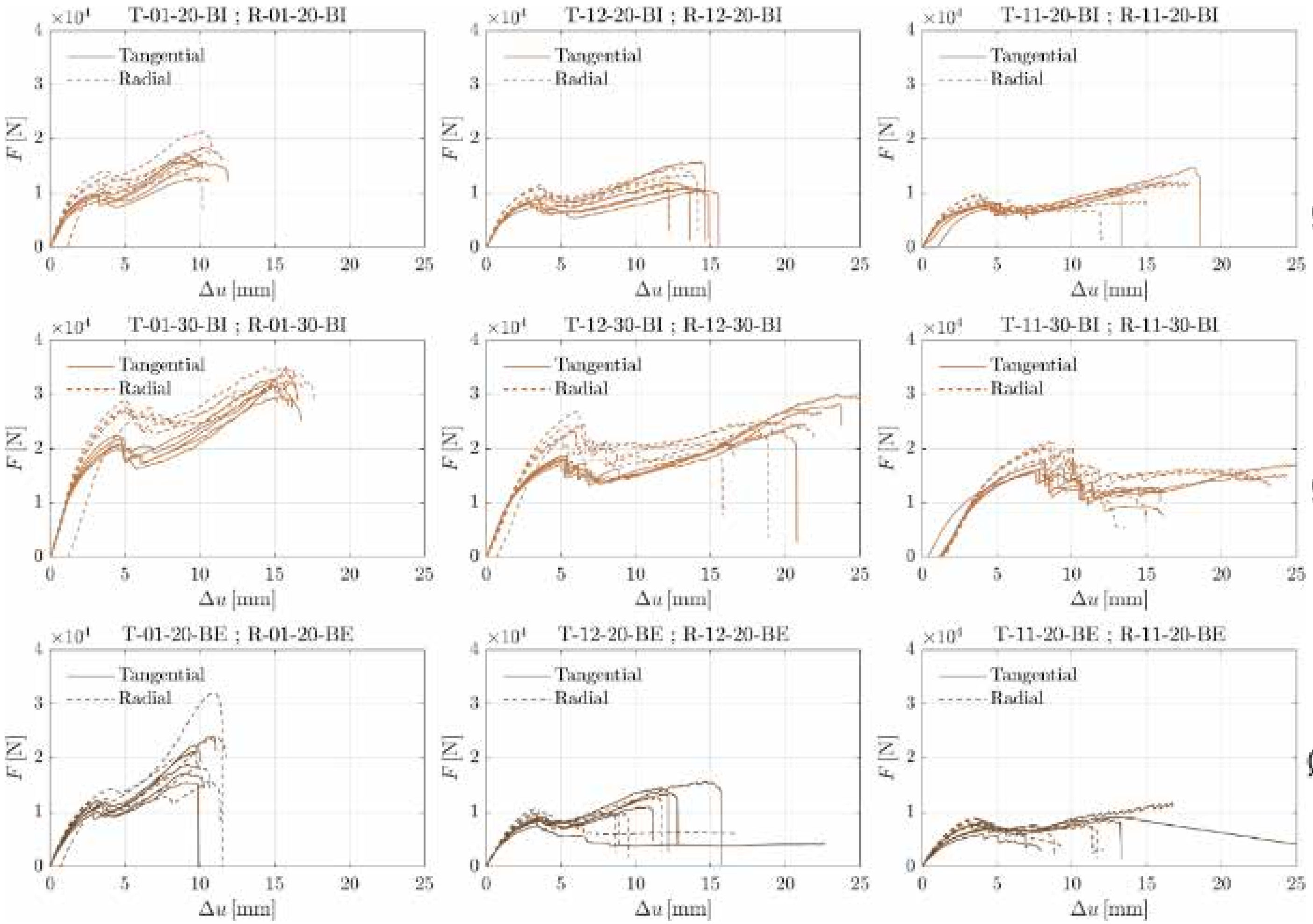

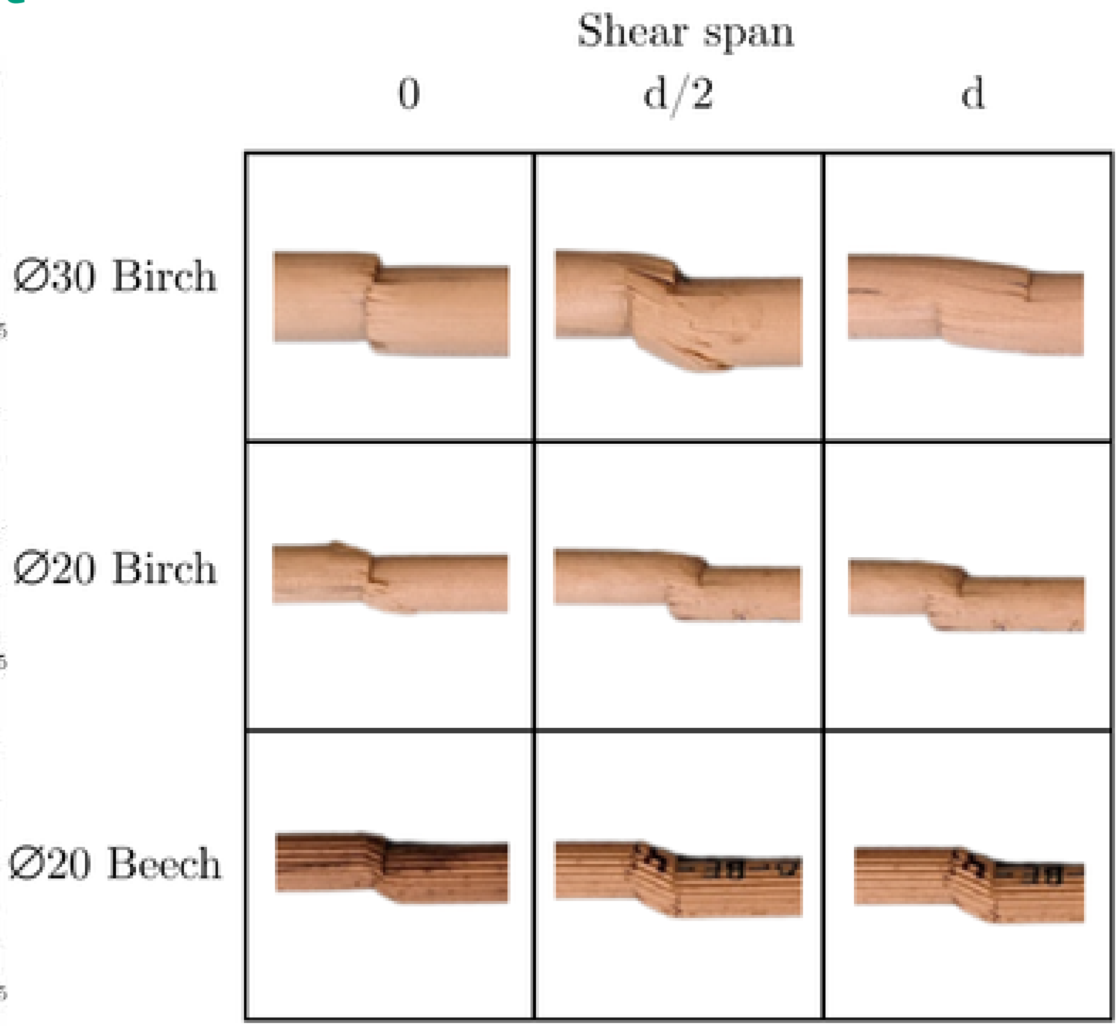

The double-peaked shape is typical of Mode-V dowels with short spans ($L_{free} \leq d/2$)

4. KTH Experimental campaign. Shear test

Group	$\bar{f}_{y,v}$ (MPa)	s_f (MPa)	Group	$\bar{f}_{y,v}$ (MPa)	s_f (MPa)
T-0/1-20-BI	18.89	1.31	R-0/1-20-BI	24.55	1.78
T-1/2-20-BI	16.20	1.20	R-1/2-20-BI	20.44	1.65
T-1/1-20-BI	14.39	0.91	R-1/1-20-BI	17.06	1.58
T-0/1-30-BI	16.14	1.23	R-0/1-30-BI	24.94	0.80
T-1/2-30-BI	15.77	0.56	R-1/2-30-BI	21.25	1.82
T-1/1-30-BI	13.60	0.95	R-1/1-30-BI	17.07	0.98
T-0/1-20-BE	23.02	2.12	R-0/1-20-BE	25.00	3.17
T-1/2-20-BE	18.06	1.62	R-1/2-20-BE	21.21	1.43
T-1/1-20-BE	14.48	1.95	R-1/1-20-BE	18.91	3.05

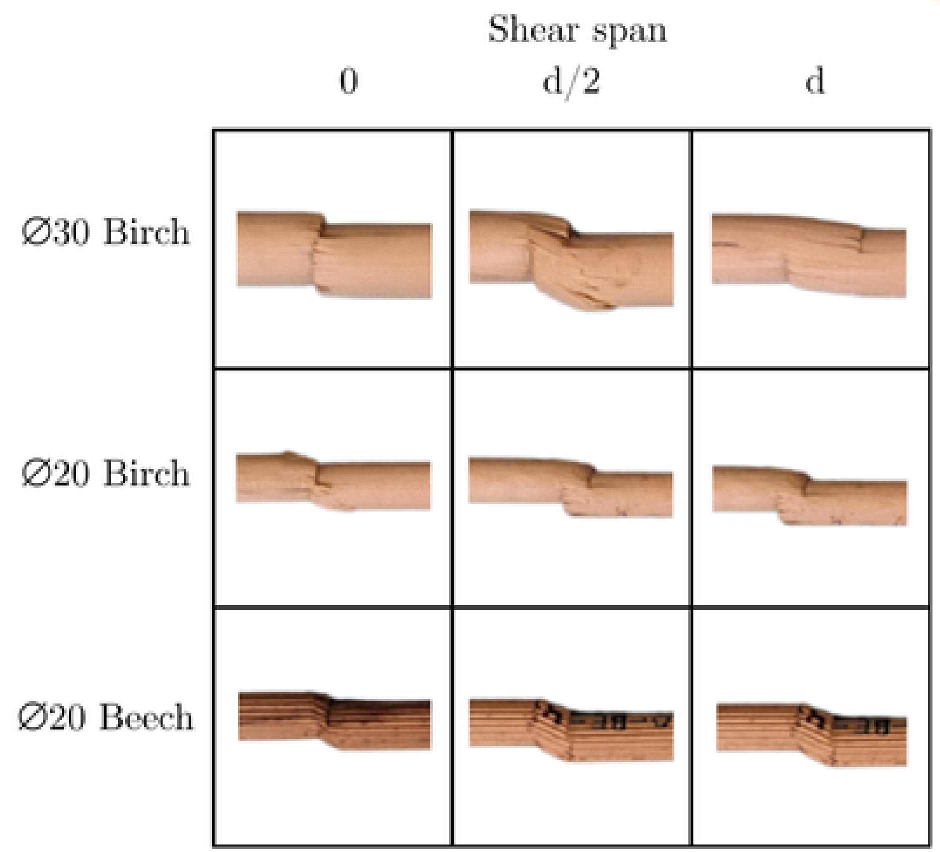

- Radial loading consistently gives higher shear capacity than tangential loading for the same span ratio and diameter;
- Increasing the free shear span from 0 to 1.0d lowers the mean strength by roughly 25–30%;
- Beech dowels outperform birch under identical test conditions, reflecting their higher density and stiffness.

4. KTH Experimental campaign. Insights for possible dynamic grading...

free–free boundary conditions while reducing support vibration

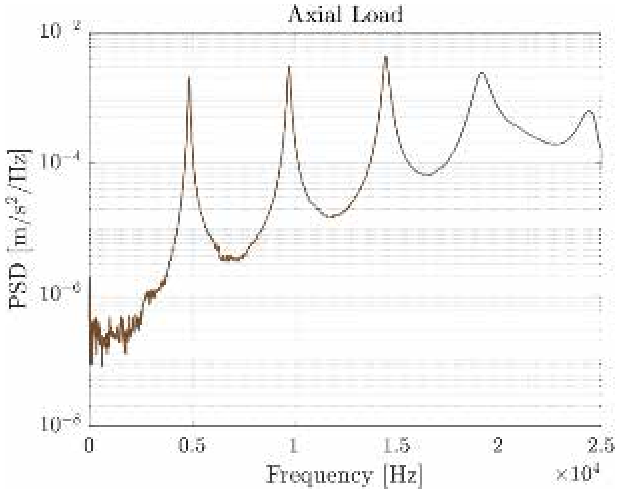

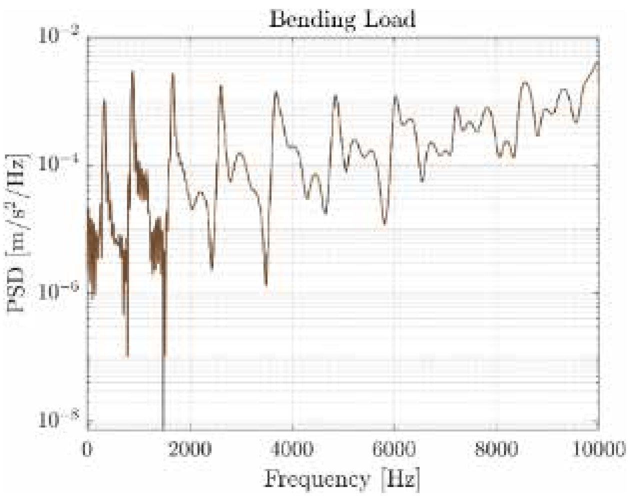

peak-picking clearly identifies axial frequencies and provides at least seven bending modes

miniature accelerometer attached with beeswax

axial modes

bending about the tangential axis

4. KTH Experimental campaign. Insights for possible dynamic grading...

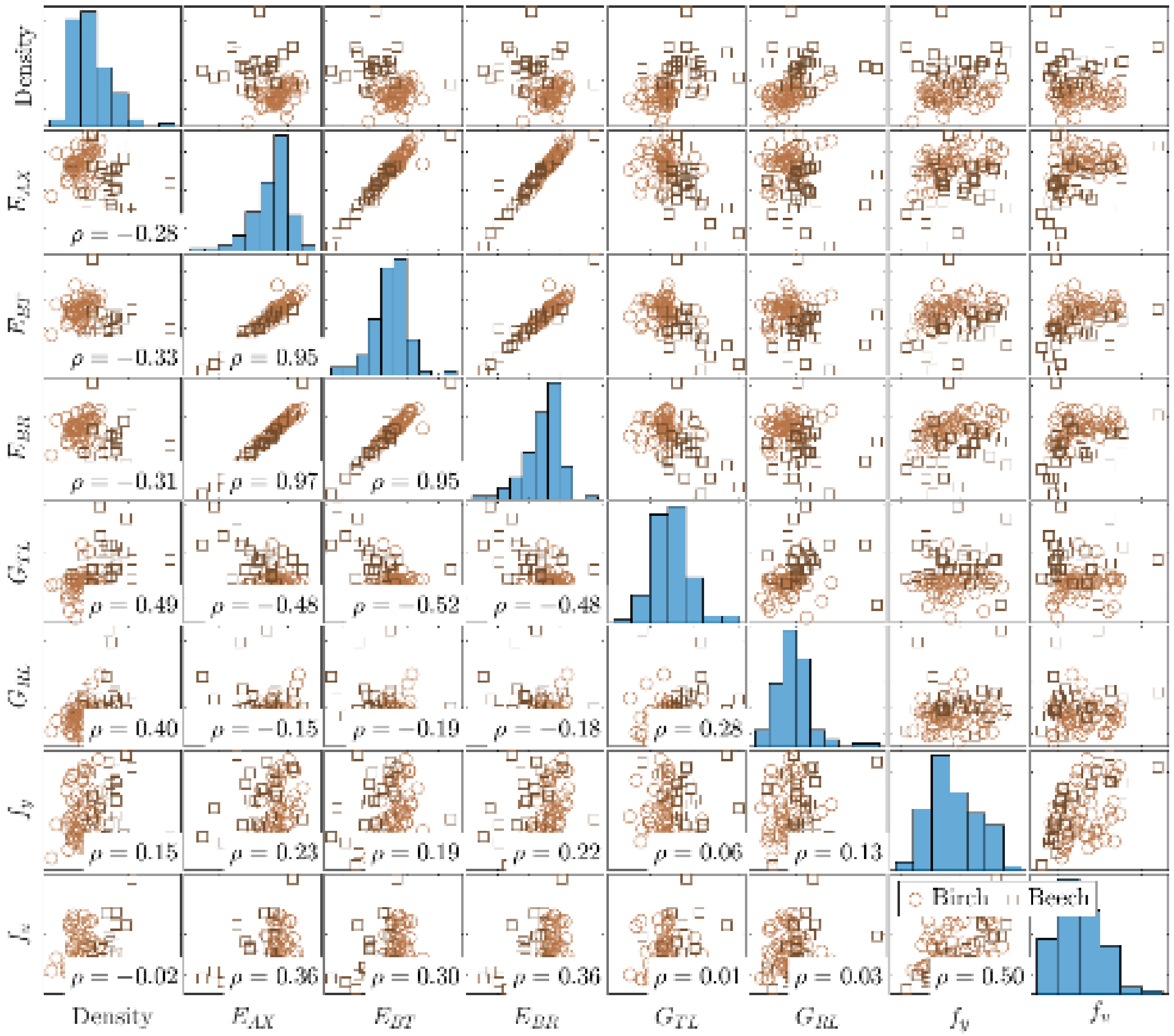

	Density	E_{AX}	E_{BT}	E_{BR}	G_{TL}	G_{RL}	f_y	f_u
All specimens								
Density	1	−0.28	−0.33	−0.31	0.49	0.40	0.15	−0.02
E_{AX}	−0.28	1	0.95	0.97	−0.48	−0.15	0.23	0.36
E_{BT}	−0.33	0.95	1	0.95	−0.52	−0.19	0.19	0.30
E_{BR}	−0.31	0.97	0.95	1	−0.48	−0.18	0.22	0.36
G_{TL}	0.49	−0.48	−0.52	−0.48	1	0.28	0.06	0.01
G_{RL}	0.40	−0.15	−0.19	−0.18	0.28	1	0.13	0.03
f_y	0.15	0.23	0.19	0.22	0.06	0.13	1	0.50
f_u	−0.02	0.36	0.30	0.36	0.01	0.03	0.50	1
Birch only								
Density	1	0.36	0.25	0.34	0.17	0.44	0.23	−0.02
E_{AX}	0.36	1	0.91	0.98	0.06	0.31	0.40	0.31
E_{BT}	0.25	0.91	1	0.93	−0.01	0.19	0.36	0.34
E_{BR}	0.34	0.98	0.93	1	0.06	0.24	0.45	0.38
G_{TL}	0.17	0.06	−0.01	0.06	1	0.18	0.06	0.22
G_{RL}	0.44	0.31	0.19	0.24	0.18	1	0.12	0.02
f_y	0.23	0.40	0.36	0.45	0.06	0.12	1	0.31
f_u	−0.02	0.31	0.34	0.38	0.22	0.02	0.31	1
Beech only								
Density	1	0.06	−0.07	0.02	0.06	−0.07	0.04	0.18
E_{AX}	0.06	1	0.94	0.94	−0.46	−0.03	0.28	0.41
E_{BT}	−0.07	0.94	1	0.94	−0.51	−0.05	0.21	0.26
E_{BR}	0.02	0.94	0.94	1	−0.40	−0.02	0.23	0.36
G_{TL}	0.06	−0.46	−0.51	−0.40	1	−0.08	−0.04	−0.02
G_{RL}	−0.07	−0.03	−0.05	−0.02	−0.08	1	0.10	0.15
f_y	0.04	0.28	0.21	0.23	−0.04	0.10	1	0.77
f_u	0.18	0.41	0.26	0.36	−0.02	0.15	0.77	1

4. Mode V. Empirical capacity model with two regressors

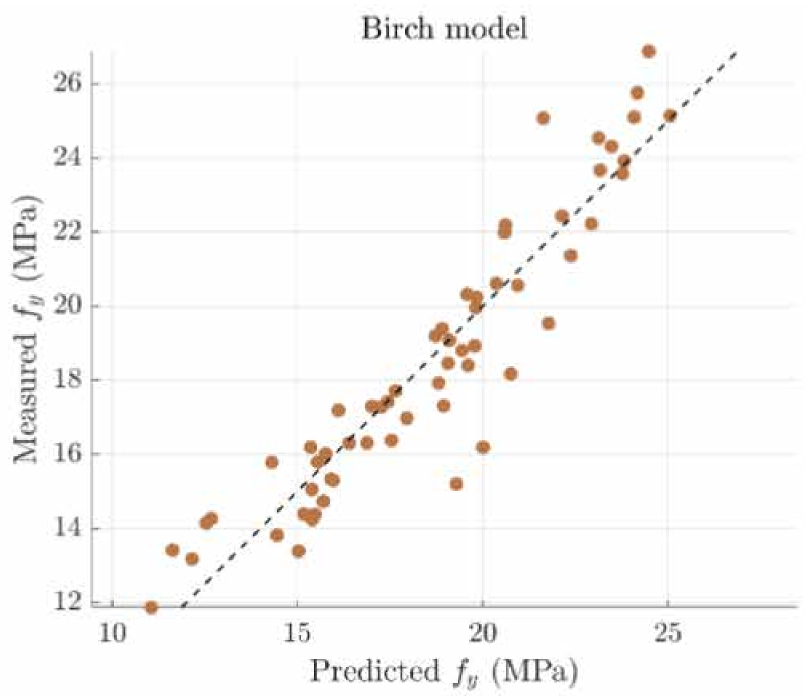

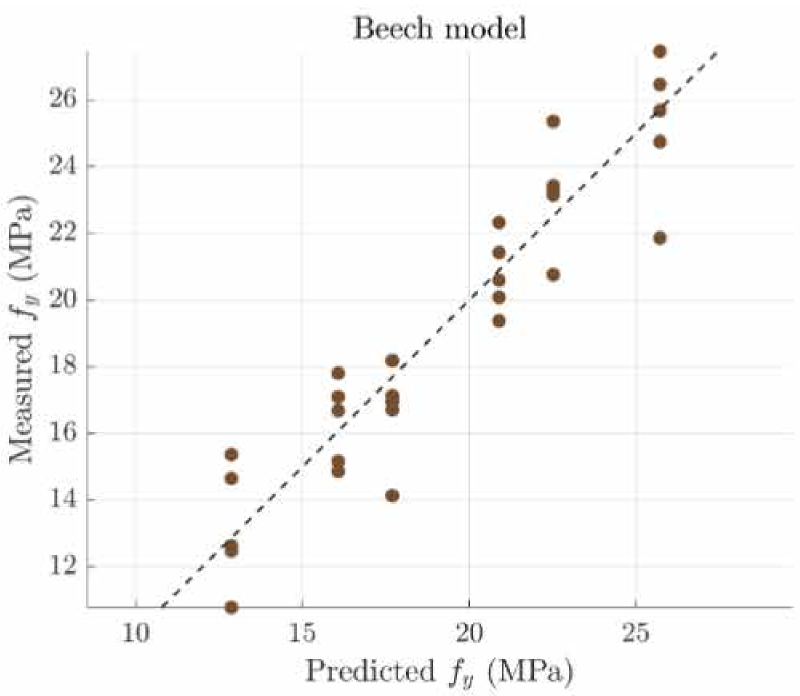

$$\widehat{f}_{y,\text{Birch}} = 19.03 - 0.227\,\text{Gap}_{\text{mm}} + 4.714\,D_{\text{R}} \qquad (\text{MPa; 5-fold RMSE} = 1.50\ \text{MPa})$$

$$\widehat{f}_{y,\text{Beech}} = 22.521 - 0.483\,\text{Gap}_{\text{mm}} + 3.202\,D_{\text{R}} \qquad (\text{MPa; 5-fold RMSE} = 1.37\ \text{MPa})$$

4. Mode V. Alternative interaction model

Bending-shear interaction model for Mode-V dowel failure

$$M = \frac{FL}{4}, \qquad V = \frac{F}{2}.$$

$$\sigma_{\max} = \frac{32M}{\pi d^3} = \frac{8FL}{\pi d^3}, \qquad \tau_{\max} = \frac{4V}{3A} = \frac{8F}{3\pi d^2}.$$

$$\left(\frac{\tau_{\max}}{f_v}\right)^{n_1} + \left(\frac{\sigma_{\max}}{f_m}\right)^{n_2} = 1$$

$$\left[\frac{8F/(3\pi d^2)}{f_v}\right]^{n_1} + \left[\frac{8FL/(\pi d^3)}{f_m}\right]^{n_2} = 1$$

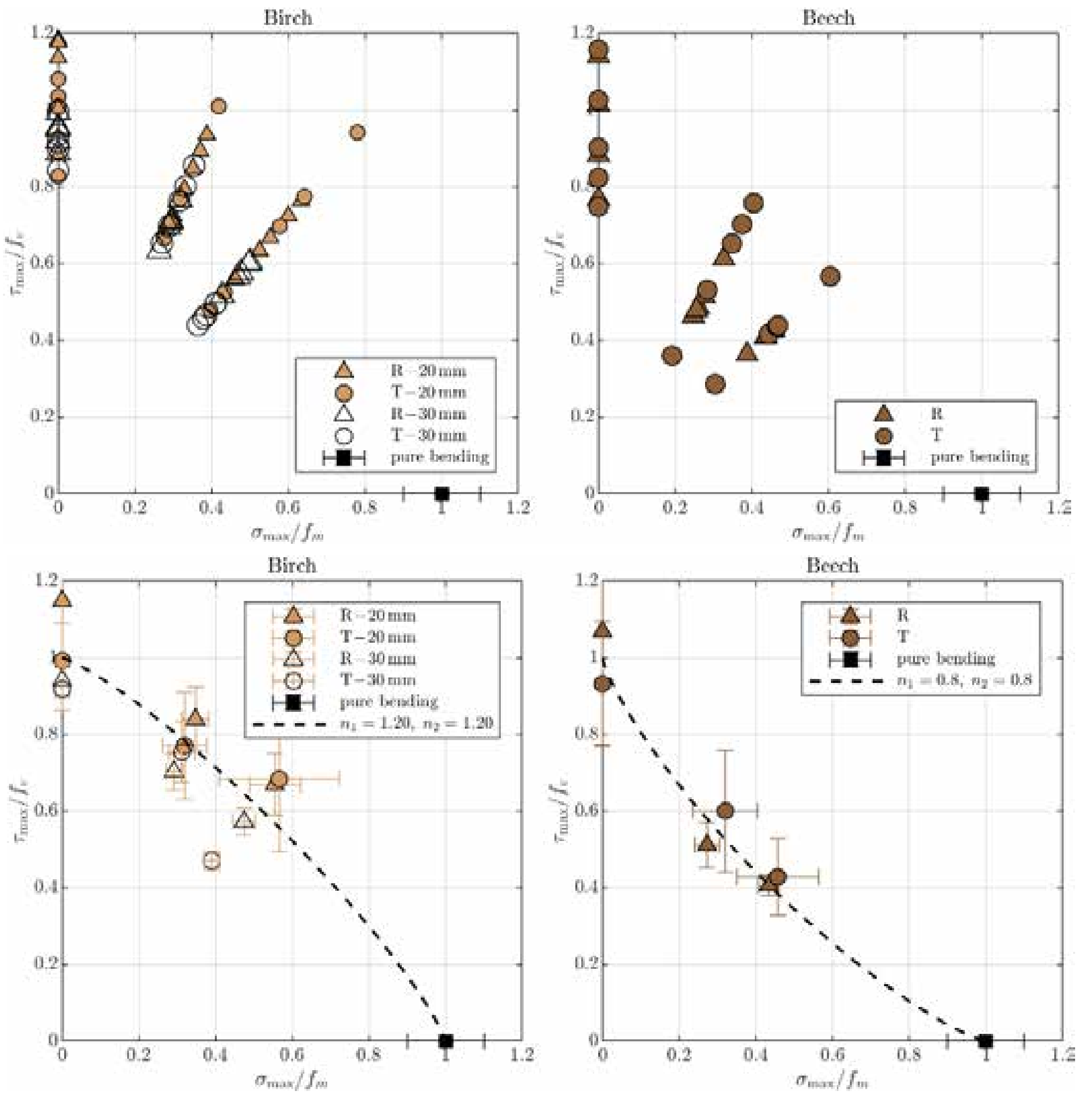

normalised Mode-V stress states of all specimens

4. Mode V alternative model

$$\frac{\tau_{\max}}{f_v} + \frac{\sigma_{\max}}{f_m} = 1$$

An almost linear domain confirms the absence of plastic hinges. A quadratic or otherwise convex envelope is typical when significant inelastic redistribution occurs.

Mechanical meaning of the interaction-domain shape.

Envelope shape	Dominant mechanism	Typical for
Linear, Eq. (20)	Independent shear and bending failure / brittle rupture; no plastic hinge; fracture triggered by the first stress component reaching its limit.	Hardwood dowels (Mode V), concrete punch-shear, brittle masonry.
Quadratic or convex, $\tau^{n_1} + \sigma^{n_2} = 1$, $n_i > 1$	Interactive failure; inelastic redistribution and plastic-hinge formation; synergy between stress components.	Steel bolts in timber (Johansen Modes a–f), ductile steel beams, tough composites.

4. Mode V alternative model

Possible design format

$$\tau / f_v + \sigma / f_m = 1 \qquad \tau_{\max} = \frac{8V}{3\pi d^2}, \qquad \sigma_{\max} = \frac{8V}{\pi d^2}.$$

$$\longrightarrow V_{\text{int}} = \frac{3\pi d^2}{8(1+3f_v/f_m)} f_v \longrightarrow V_{R,k} = \min\{V_{\text{int}},\ f_v A_s,\ f_{h,1}t_{h,1},\ 0.5\, f_{h,2}t_{h,2}\}$$

Dowel	d [mm]	f_m [MPa]	f_v [MPa]	V_{pred} per dowel [kN]	V_{exp} per dowel [kN]	Rel. error [%]
Birch	20.00	132.70	16.49	5.66	5.32	6.40

Journal papers on wooden dowels

Contents lists available at ScienceDirect

Engineering Structures

journal homepage: www.elsevier.com/locate/engstruct

Mechanical performance of pure-wood moment-resisting ridge joints with plywood gussets and wooden dowels

Angelo Aloisio [a,b,*], Yue Wang [c], Roberto Crocetti [c], Anders Q. Nyrud [a], Roberto Tomasi [a]

[a] Faculty of Science and Technology, Norwegian University of Life Sciences, Norway
[b] Department of Civil Engineering, University of L'Aquila, Italy
[c] Department of Civil and Architectural Engineering, The Royal Institute of Technology, Stockholm, Sweden

Contents lists available at ScienceDirect

Engineering Structures

journal homepage: www.elsevier.com/locate/engstruct

Fire resistance of wooden dowelled cross-laminated timber panels under in-plane loading

Angelo Aloisio [a,*,1], Dag Pasquale Pasca [b,1], Massimo Fragiacomo [a,1]

[a] Department of Civil, Construction-Architectural and Environmental Engineering, Università degli Studi dell'Aquila, L'Aquila, Italy
[b] Norsk Treteknisk Institutt (Norwegian Institute of Wood Technology), Oslo, Norway

Contents lists available at ScienceDirect

Construction and Building Materials

journal homepage: www.elsevier.com/locate/conbuildmat

Sensitivity of bending stiffness to moisture content in adhesive-free wooden-doweled cross-laminated timber panels

Angelo Aloisio [a,*], Dag Pasquale Pasca [b], Roberto Tomasi [c], Massimo Fragiacomo [a]

[a] Department of Civil, Construction-Architectural and Environmental Engineering, Università degli Studi dell'Aquila, L'Aquila, Italy
[b] Norsk Treteknisk Institutt (Norwegian Institute of Wood Technology), Oslo, Norway
[c] Faculty of Science and Technology, Norwegian University of Life Sciences, Norway

Contents lists available at ScienceDirect

Construction and Building Materials

journal homepage: www.elsevier.com/locate/conbuildmat

Experimental and analytical investigation on timber connections with beech, birch and laminated densified wooden dowels

Roberto Tomasi [a,*], Yuri De Santis [c], Angelo Aloisio [c,a], Roberto Crocetti [d], Vegard H. Sæby [a], Anders Q. Nyrud [b]

[a] Faculty of Science and Technology, Norwegian University of Life Sciences, Norway
[b] Faculty of Environmental Sciences and Natural Resource Management, Norwegian University of Life Sciences, Norway
[c] Department of Civil, Construction-Architectural and Environmental Engineering, Università degli Studi dell'Aquila, L'Aquila, Italy
[d] Department of Civil and Architectural Engineering, The Royal Institute of Technology, Stockholm, Sweden

3. Conclusion

- Combined free–free modal tests with quasi-static double-shear experiments on birch (20, 30mm) and beech (20mm) dowels to clarify the mechanics of Mode-V failure.
- Birch showed higher axial/bending moduli (about 18–19 GPa) than beech (about 15–16 GPa), but elastic moduli had weak, non-practical correlation with shear strength.
- Normalised stress states align with an almost linear bending–shear interaction. This points to negligible interaction reserve, no stable plastic hinge, and a brittle, parallel-to-grain shear fracture governed by whichever action reaches its limit first.
- Mode-V capacity of hardwood dowels can be checked with a simple additive bending–shear criterion and the two-parameter span/direction model; treat it as a design-oriented, physics-consistent alternative to plastic-hinge assumptions.
- Calibration covered one aluminium embedment, two diameters, and near-12% moisture content. Extensions to timber or steel plates, other MC, and broader size ranges require targeted testing.

Thank you for your attention